CHAPTER 4

RESULTS AND DISCUSSIONS

4.1. Introduction

This chapter presents the results and data analyses which include results of the material characterization and also hydrogen adsorptions involved in the study. Additionally, the results that were obtained are discussed in reference to other previous work and literature. In order to highlight the findings from the study, the results are generally presented as tables and figures.

4.2. X-Ray Diffraction (XRD) Results

4.2.1. XRD of As-synthesized Mg-Al HTlcs

Figure 4.1shows the XRD patterns of the synthesized Mg-Al HTlcs. It was found from the powder XRD results that the solids with Mg/Al molar ratio of two, three and four produced hydrotalcite structures. They are similar to the XRD patterns for hydrotalcites obtained from previous studies [19], [130], which showed sharp and symmetric peaks at low 2θ angles and broad and asymmetric ones at higher 2θ angles, characteristics of clay materials with a layered structure [18], [20].

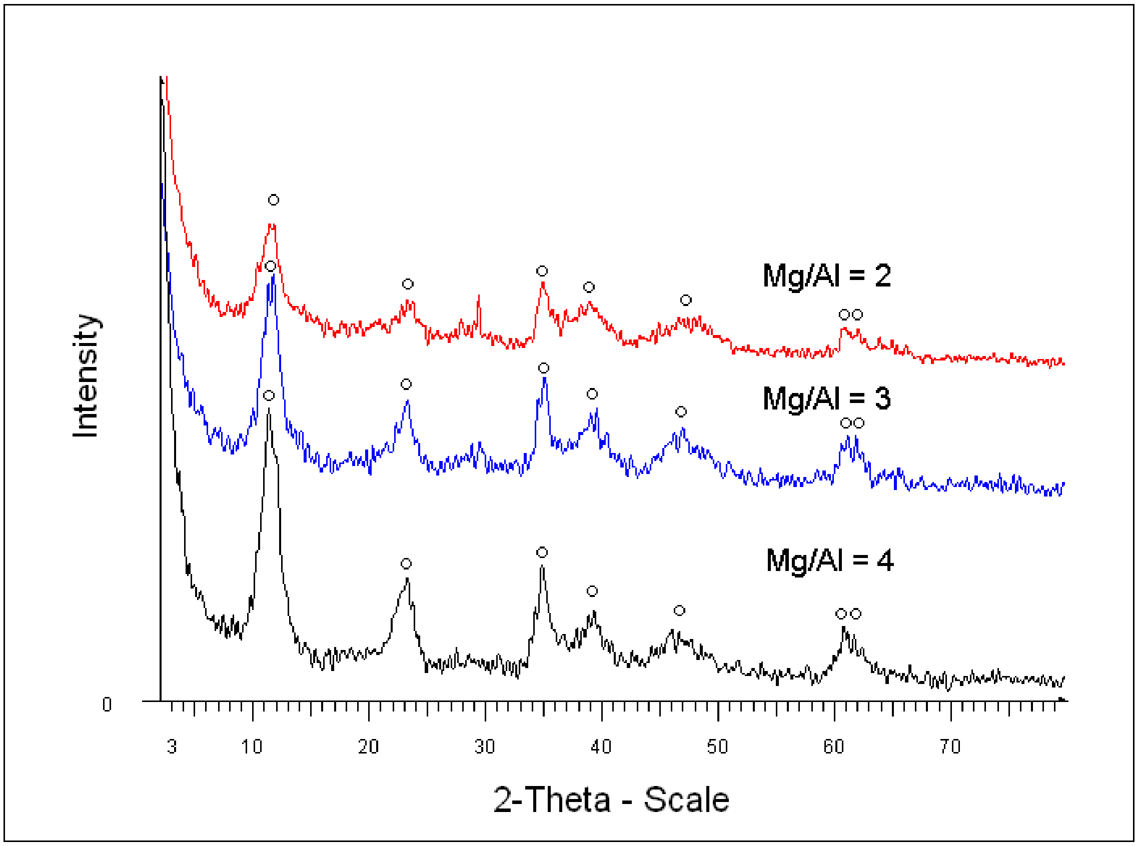

Figure 4.1: The XRD patterns of Mg-Al HTlcs, Mg/Al molar ratio 2, 3 and 4: (○) Hydrotalcite

As shown in Figure 4.1, the sharp peaks at 2θ angles of about 11°, 22° and 35° corresponds to the (003), (006) and (009) crystal planes respectively, indicating crystalline layered structure. Furthermore, the broad and asymmetric peaks at lower 2θ angles of about 38° and 46° can be attributed to the (015) and (018) crystal planes which are characteristics of hydrotalcites [24]. Additionally, the two peaks just over 60° may correspond to the (110) and (113) crystal planes of hydrotalcite (SS-NNN PDF 89-0460) [20], [131].

Furthermore, the values of the d-spacing (basal spacing) of the highest peak for all three materials are close to 7.6Å which indicates that the samples have hydrotalcite like structure with carbonate anions in the interlayer [17]. Apart from that, the minimum M^{2+}/M^{3+} molar ratio has to be 2:1 to attain the hydrotalcite-like structure.

The limitation of the M^{2+}/M^{3+} molar ratio was observed in previous studies where pure HTlcs was only producible between the Mg/Al molar ratio of 1.9 and 3.1 [68].

The peak intensity or sharpness is also related to sample crystallinity. Observations of the XRD pattern in Figure 4.1 showed that increasing the Mg/Al molar ratio increases the peak intensity and this indicates that the crystallinity is increased with higher Mg content [16], [95], [131].

4.2.2. XRD of Calcined Mg-Al HTlcs

The XRD patterns of calcined Mg-Al HTlcs are illustrated in Figure 4.2 and Figure 4.3, for the calcination temperatures of 450°C and 600°C respectively. It can be seen in Figure 4.2 that for Mg-Al HTlcs with Mg-Al molar ratio of two and three, there are peaks at 2θ values of 29.5° and 30°. These new peaks can be attributed to the presence of of $NaNO_3$ (nitratine) (SS-NNN PDF 89-2828) in the sample [132]. This is probably caused by the remnants of sodium from the synthesis solution.

Figure 4.2 also indicates that the Mg-Al HTlcs with Mg/Al molar ratio of two was completely calcined at 450°C and it has lost the hydrotalcite structure. However, in the calcined Mg-Al HTlcs with Mg/Al molar ratio of three and four the hydrotalcite structure is maintained as the peaks which correspond to the hydrotalcite structure are still present. This is also observed for Mg-Al HTlcs calcined at 600°C (Figure 4.3).

The preservation of the hydrotalcite structure after calcination has also been reported in previous work [98]. The hydrotalcite structure is still present in the calcined sample due to the rehydration of the sample prior to testing. The rehydration occurs due to the ‘memory effect’ of the hydrotalcite material where reconstitution of the decomposed material occurs when exposed to water or water vapour under. During this process, any anion present in the surrounding medium will be intercalated into the HTlc but this property was found in previous researches to be limited to HTlcs calcined at temperatures below 500°C [65] [133].

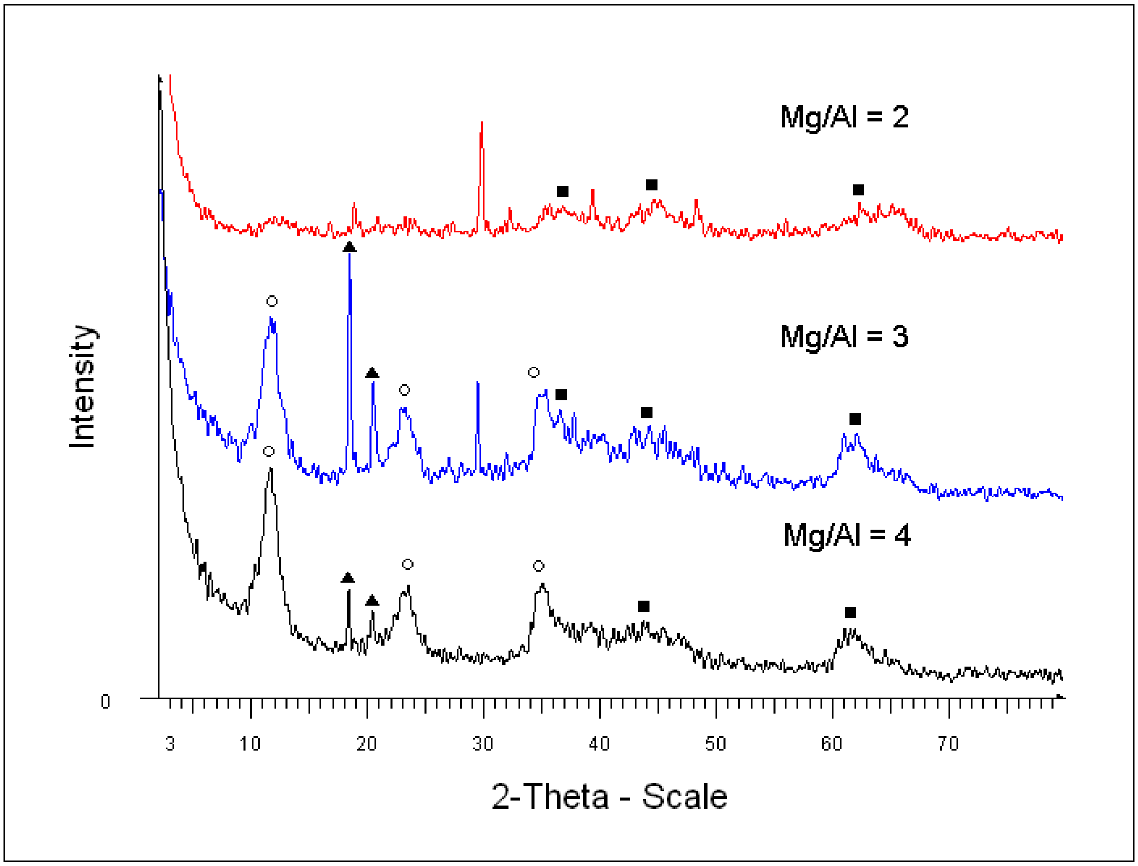

Figure 4.2: The XRD patterns of Mg-Al HTlcs calcined at 450°C, Mg/Al molar ratio 2, 3 and 4: (○) Hydrotalcite, (■) MgO, (▲) Gibbsite

Observation of Figure 4.2 and 4.3 showed that in the calcined Mg-Al HTlcs, in addition to peaks corresponding to HTlcs, there are other peaks at 37°, 43° and 62 °. These peaks can be attributed to the mixed magnesium oxide MgO (SS-NNN PDF 01-1235) [24] [100]. This is in agreement with a previous study by Labajos et al. [131] where it was found that calcination of Mg-Al HTlcs will lead to its decomposition and finally MgO and $MgAl_2O_4$ will be formed. Additionally, the Mg-Al HTlcs with Mg/Al molar ratio of three and four when calcined at 450°C, showed new peaks at 2θ angles of 18° and 21°. These peaks can also be observed for Mg-Al HTlcs calcined at 600°C (Figure 4.3), and they can be attributed to gibbsite ($Al_2O_3.3H_2O$) [107]. Apart from the formation of mixed oxides, the figures above still show that the HTlc structure is retained even after calcination and this may be caused by the rehydration of the materials during testing [100].

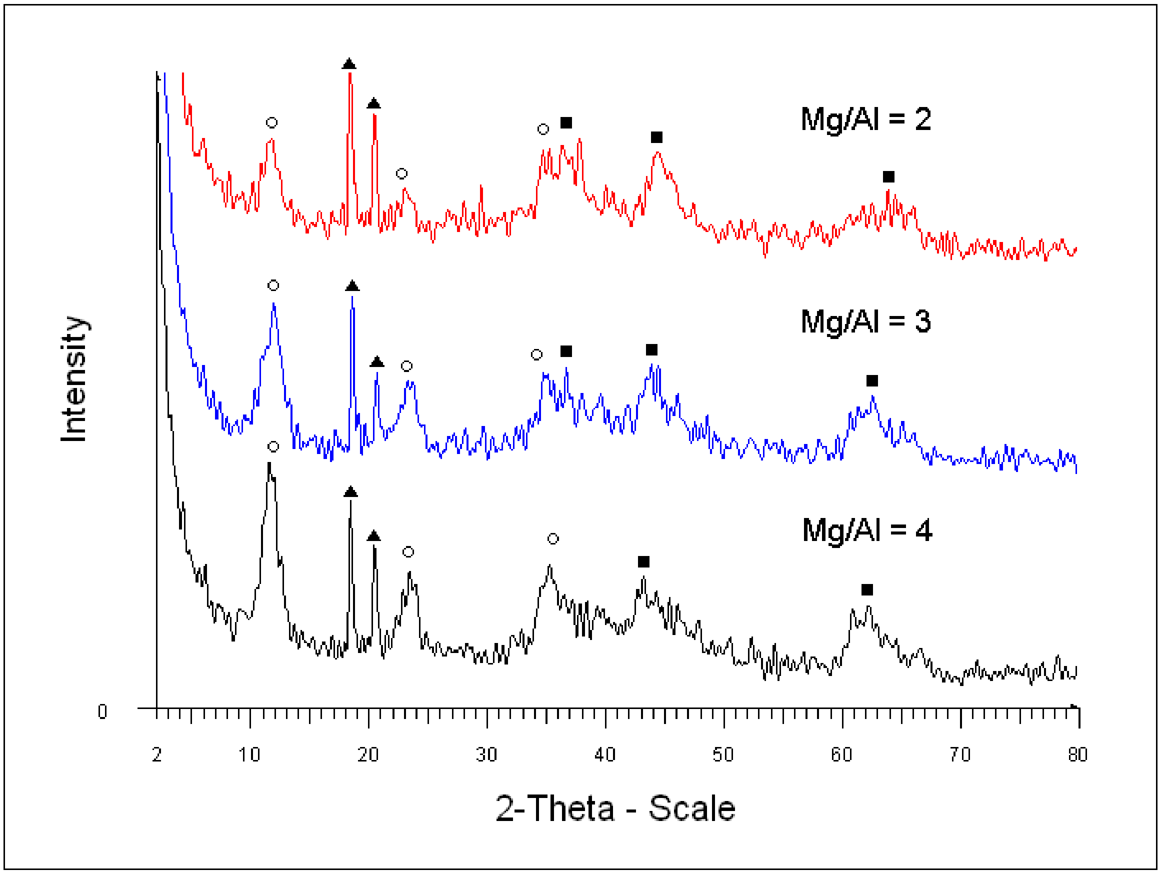

Figure 4.3: The XRD patterns of Mg-Al HTlcs calcined at 600°C, Mg/Al molar ratio 2, 3 and 4: (○) Hydrotalcite, (■) MgO, (▲) Gibbsite

Based on Figures 4.2 and 4.3, it can be seen that the peak height of the metal oxide peaks for most samples increased as calcination temperature is increased from 450°C to 600°C. This result agrees with results of Olsbye et al. [71] where as calcination temperature is increased, MgO crystal growth is also accelerated. Similar to the uncalcined Mg-Al HTlcs, the calcined samples exhibited sharper peaks at higher Mg/Al ratio indicating better crystallinity with increasing Mg content [134]-[136].

The Figures 4.4 and 4.5 present the XRD pattern for the Mg-Al HTlcs calcined at 750°C and 900°C. It can be from the XRD pattern that the characteristics hydrotalcite peaks have disappeared after calcination at these high temperatures indicating destruction of the hydrotalcite layered structure. Additionally, at 2θ angles of 37°, 43° and 62° new peaks attributable to MgO (SS-NNN PDF 01-1235) are present. This observation indicates that mixed oxides are also formed at high calcination temperatures. Meanwhile, the peak at 2θ angle of 30° can be attributed to spinel ($MgAl_2O_4$) (SS-NNN PDF 02-1086).

For figure 4.4 and 4.5, the increment of Mg/Al ratio first increased with Mg/Al content before decreasing when the Mg/Al molar ratio equals to 4. It can also be seen from both figures (4.4 and 4.5) that for Mg-Al HTlcs with molar ratio of three and four (calcined at 750°C and 900°C), the peaks for MgO are sharper compared to that in the Mg-Al HTlcs calcined at 450°C and 600°C indicating higher crystallinity. As before, this is due to the acceleration of MgO crystal growth at increasing calcination temperatures [71].

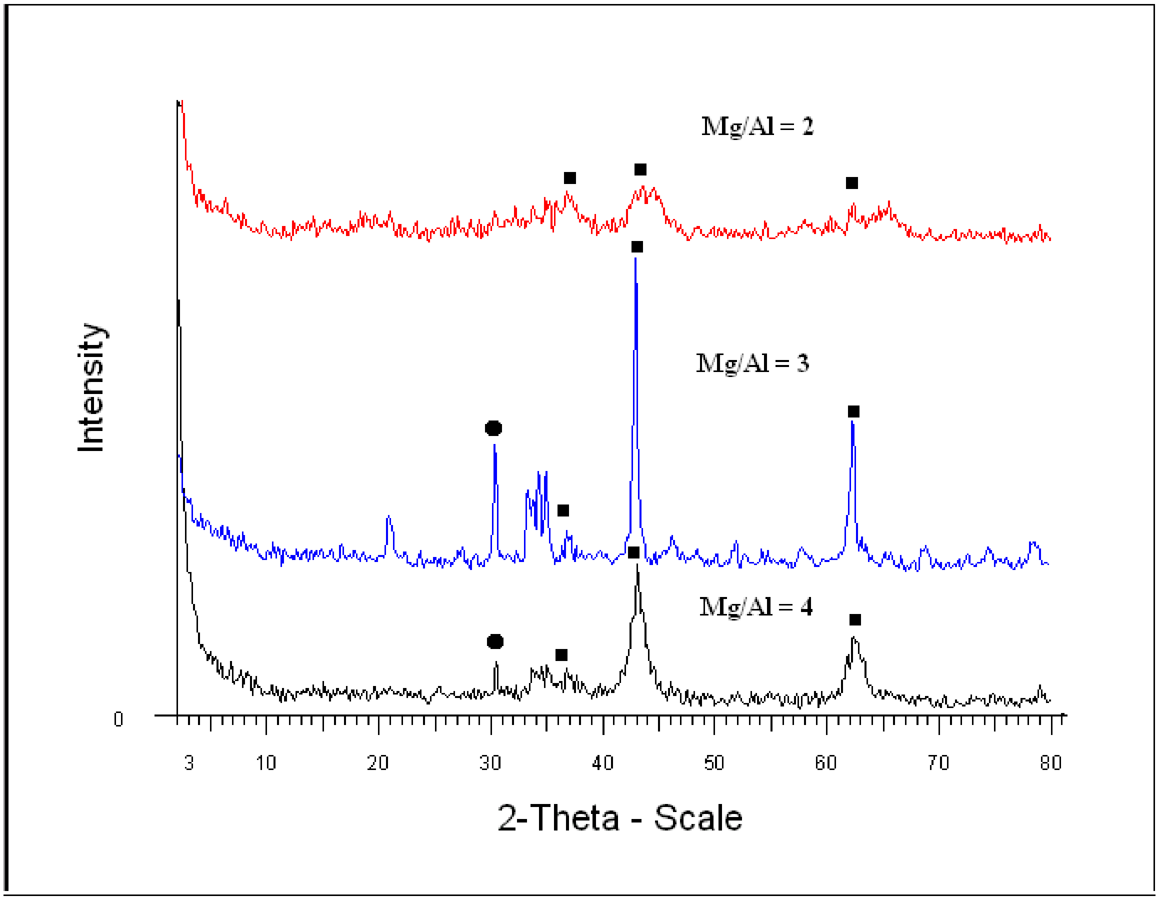

Figure 4.4: The XRD patterns of Mg-Al HTlcs calcined at 750°C, Mg/Al molar ratio 2, 3 and 4: (○) Hydrotalcite, (■) MgO, (●) Spinel ($MgAl_2O_4$)

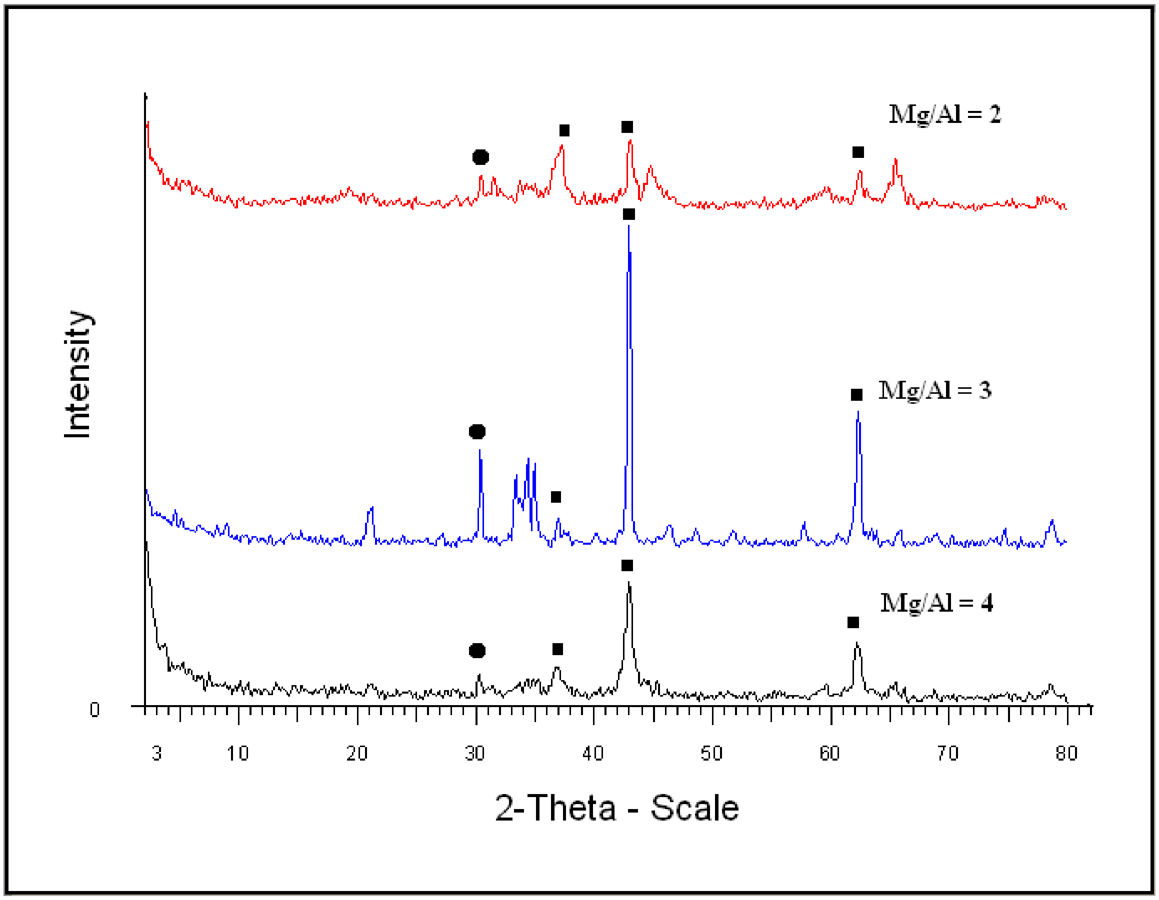

Figure 4.5: The XRD patterns of Mg-Al HTlcs calcined at 900°C, Mg/Al molar ratio 2, 3 and 4: (○) Hydrotalcite, (■) MgO, (●) Spinel ($MgAl_2O_4$)

Additionally, the calcination also decreases the (003) basal spacing of the calcined samples and the weight loss of both samples calcined at 450°C and 600°C was determined to be 40 percent which is in agreement with previous studies [17] [90]. Besides that, the basal spacings of the as-synthesized and calcined samples were also found to increase with higher Mg content. This observation agrees with the decreased Coulombic attractive forces between the positively charged brucite-like layers and the negatively charged anions in the interlayer region [133].

4.2.3. XRD of As-synthesized Ni-Mg-Al HTlcs

The Ni-Mg-Al HTlcs with Ni/Mg/Al molar ratios of 1:2:1 and 2:1:1 were also characterized using XRD in order to determine the species present in the samples. The XRD patterns of both samples are presented in Figure 4.6. As illustrated in Figure 4.6, both samples exhibit peaks that can be attributed to hydrotalcites which are at 2θ angles of 11°, 22°, 35°, 38° and 46° (SS-NNN PDF 14-0191). This result is similar to the Mg-Al HTlcs and has been found in previous research on Ni-Mg-Al HTlcs [73] [101]. As shown in Figure 4.4, no other crystalline compound was identified and this suggests that isomophoric replacement of the Mg^{2+} in the brucite layers by Ni^{2+} has occurred [112], [137].

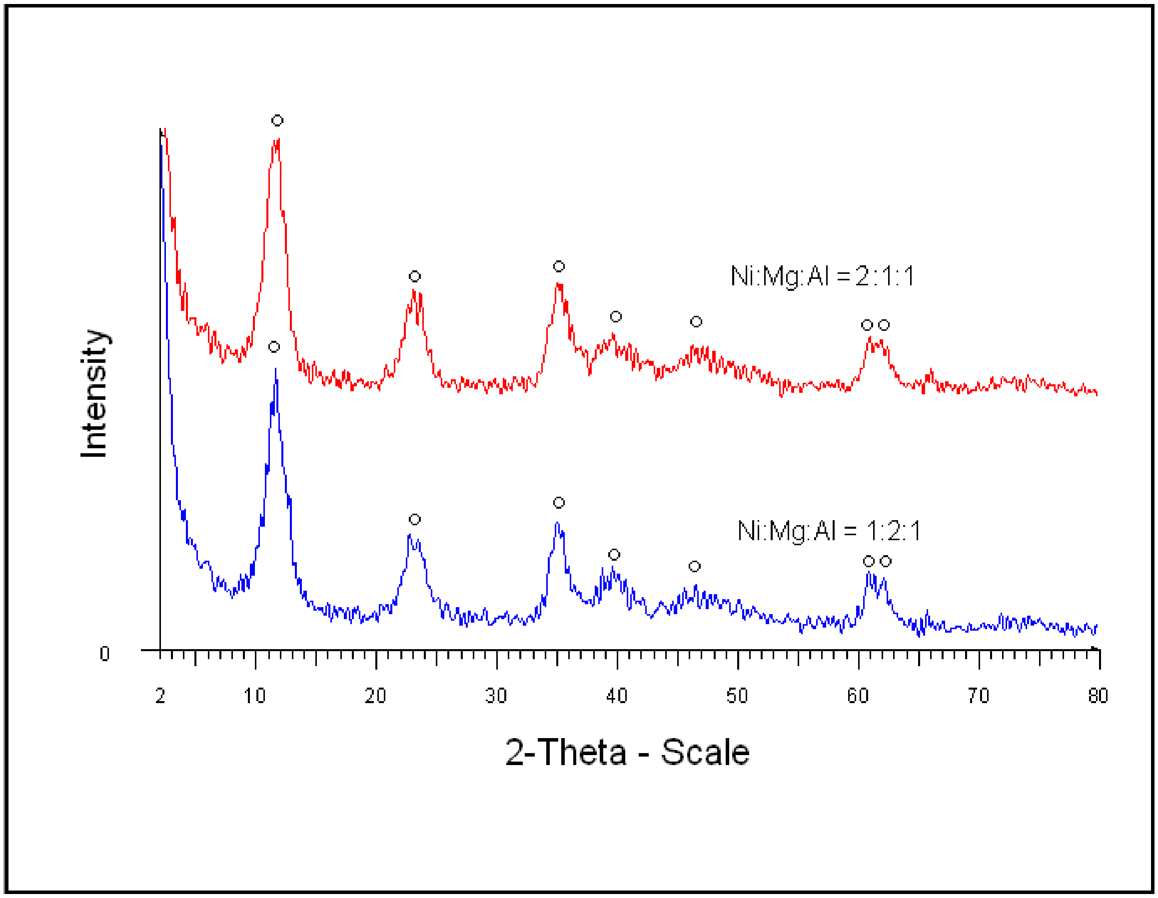

Figure 4.6: The XRD patterns for the Ni-Mg-Al HTlcs: (○) Hydrotalcite

Additionally, it can also be seen from the XRD patterns indicates that as the nickel content is increased, the sharpness of the XRD peaks are decreased indicating decrease in crystallinity of the sample [111].

4.2.4. Calcined Ni-Mg-Al HTlcs

In order to produce mixed oxides for the hydrogen adsorption process, the Ni-Mg-Al HTlcs were also calcined at temperatures 450°C and 600°C. The XRD patterns of the calcined samples are shown in Figure 4.7. It can be seen from Figure 4.7 that similar to the Mg-Al HTlcs in with Mg/Al molar ratio of two in Figure 4.2, Ni-Mg-Al HTlcs also showed the disappearance of the hydrotalcite peaks at 2θ angles of 11°, 22°, 35°, 38° and 46°. On the other hand, new broader peaks which can be ascribed to NiO and MgO (SS-NNN PDF 01-1235), (SS-NNN PDF 01-1239) are observable from the XRD patterns of the calcined material. Actually, the resulting material after calcinations is NiMg(Al)O mixed oxides since the starting material used was Ni-Mg-Al HTlcs [102].

The peaks that can be attributed to MgO and NiO are at 2θ values of 37°, 43° and 62 ° [105]. Since the ionic radii of both cations are so close (Mg^{2+}=0.86Å and Ni^{2+}=83Å in octahedral coordination) the peaks recorded for the calcined samples falls at nearly the same positions [103], [124], [132]. Furthermore, the broadness of the oxide peaks indicates low crystallinity of the calcined material due to the destruction of the layered structure.

Meanwhile, the trivalent cation (Al^{3+}) is most probably dispersed in the rock salt structure and calcination at higher temperatures will cause the crystallization of the AB_2O_4 spinel [124]. Additionally, upon calcination of the Ni-Mg-Al HTlcs at 450˚C for three hours, the initially green Ni-Mg-Al HTlcs turn to black. This is due to the formation of Ni_2O_3 during the calcination [138].

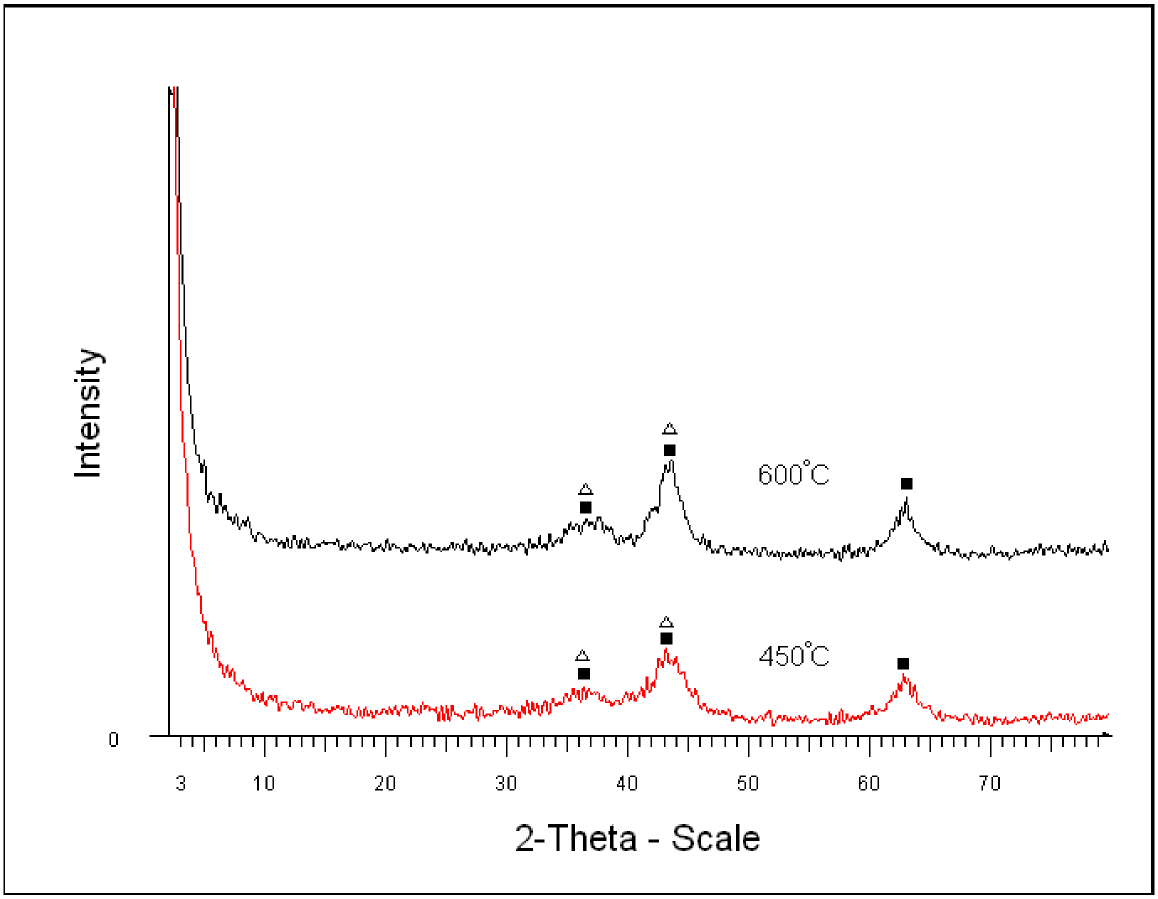

Figure 4.7: XRD pattern for Ni-Mg-Al HTlcs calcined at 600°C (top) and 450°C (bottom) with (Ni/Mg/Al molar ratio of 1:2:1, (■) MgO and (Δ) NiO

4.3. Fourier Transform Infrared (FTIR) Spectroscopy Results

4.3.1. FTIR of As-synthesized Mg-Al HTlcs

The infrared (IR) spectra of as-synthesized Mg-Al HTlcs illustrated in Figure 4.8 shows an intense broadband between 4000 and 2700cm^{-1} which represents a superimposition of deformational vibrations of physically adsorbed water, vibrations of structural OH^{-} groups, valent vibrations of OH-OH and CO_3^{2-}-OH^{-} in hydrotalcite. This broadband may also represent characteristics stretching vibration of the Mg^{2+}-OH^{-} bond in Mg, Al-hydroxy-carbonate. The band at around 1632cm^{-1} may be assigned to the adsorbed interlayer water since this is the bending vibration for δ HOH [18][106].

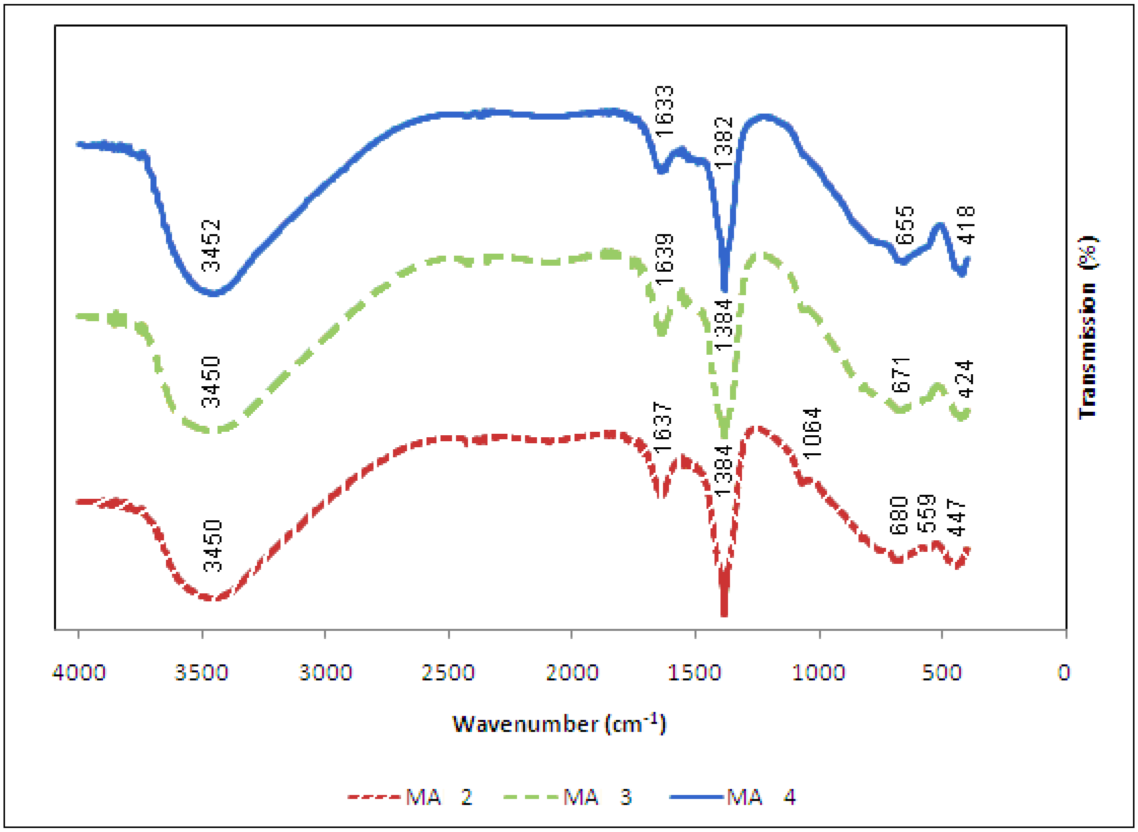

Figure 4.8: The IR spectra of as-synthesized Mg-Al HTlcs with Mg/Al molar ratio of 2 (bottom), 3 (middle) and 4 (top)

The absorption band at 1382cm^{-1} and 1384cm^{-1} may be attributed to the CO_3^{2-} absorption or the impurities of NO_3^- which is probably due to the synthesis solution [18]. In this study, the EDX analysis does not show the presence of any nitrate in the samples, therefore we can ascribe the bending at around 1380cm^{-1} only to the stretching vibration of carbonate ion [139]. The band recorded around 1300 cm^{-1} for CO_3^{2-} stretching mode is slightly shifted from that of free CO_3^{2-} at 1450cm^{-1} probably due to the restrictions experienced by carbonate anions in the interlayer. The restrictions are caused by the strong hydrogen bonding with hydroxyl sheets and interlayer water molecules [106], [107]. Thus, these FTIR results confirm the presence of interlayer carbonate and this is also determined using the assistance of EDX analysis.

The bands in the low frequency region (below 1000cm^{-1}) can be ascribed to M-OH modes [107], [140]. For instance, bands at 550 and 750 cm^{-1} can be assigned to Al-OH translation modes while the band at 650-680 cm^{-1} can be assigned to the hydroxyl translation mode influenced by Mg in the hydrotalcite structure [74]. Furthermore, the broadband around 663cm^{-1} for all three Mg-Al HTlcs have been implied as a superposition of the characteristic bonds of boehmite and hydrotalcite in this frequency interval [18].

4.3.2. FTIR of Calcined Mg-Al HTlcs

Upon calcination, the band for water at about 1632cm^{-1} still exists indicating presence of water in the material even after calcination which is due to rehydration of the materials prior to testing [19].

Additionally, a shoulder is also present at about 3000-3100cm^{-1} which is due to the bridging mode of H_2O-CO_3^{2-} [19], [66], [140]. Besides that, it can be seen for Mg-Al HTlcs with Mg/Al molar ratio of two that the broadband at 663cm^{-1} has disappeared confirming the disappearance of the hydrotalcite structure.

The IR spectra of Mg-Al HTlcs with Mg/Al molar ratio of three and four showed that some weak bands exists in the 700-600cm^{-1} wavenumber range which means that the hydrotalcite structure is still preserved. The preservation of the hydrotalcite structure of Mg-Al HTlc with Mg/Al molar ratio of three and four after calcination has also been detected by the XRD. It can also be seen that the IR spectra of both calcined Mg-Al samples are not much different from the as-synthesized samples indicating presence of the same type of anions.

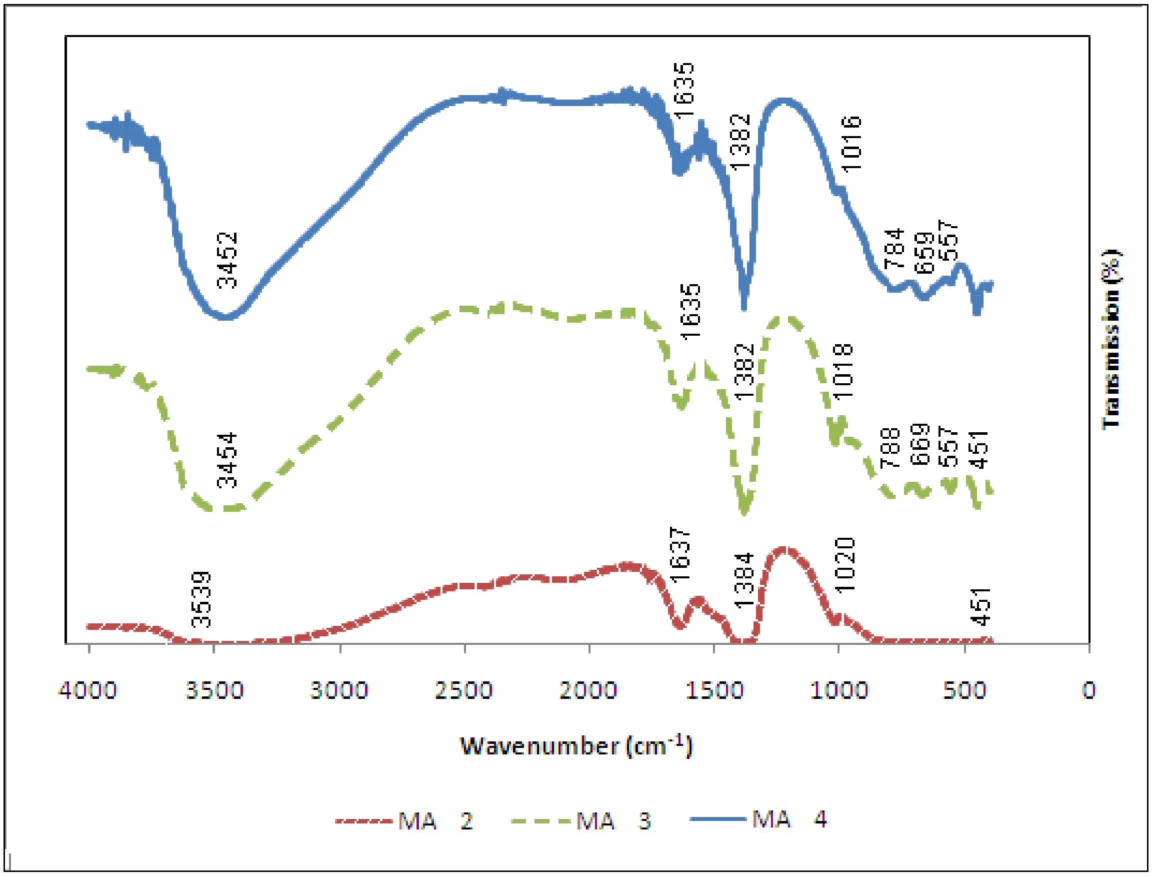

Figure 4.9: The IR spectra of Calcined Mg-Al HTlcs with Mg/Al molar ratio of 2 (bottom), 3 (middle) and 4 (top) calcined at 450°C

Besides that, it can be seen from Figure 4.9 that the IR spectra of the samples display new peaks in the low frequency 1000-400cm^{-1} region. These new peaks indicate that mixed oxides are formed since it represents the lattice vibration modes of metal oxides (M-O) and metal hydroxides (M-OH) vibrations [141]. More specifically, the bands that appear at around 788, 659 and 557cm^{-1} can be attributed to the presence of Mg-O and Al-O bands in the calcined samples [19] [139]. The bands are visible for Mg-Al HTlcs with Mg/Al molar ratio of three and four but are less pronounced for Mg-Al HTlcs with Mg/Al molar ratio of two. For comparison of the samples before and after calcination, the IR spectra of the as-synthesized and calcined Mg-Al HTlcs are presented in Figure 4.10.

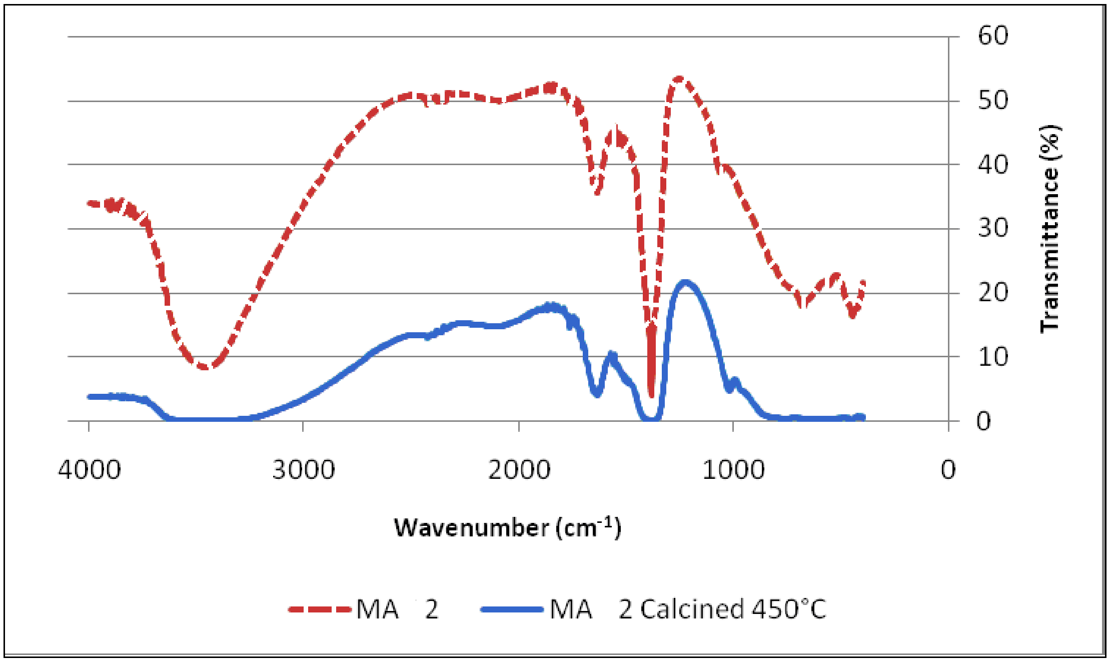

Figure 4.10: The IR spectra of as-synthesized (top) and calcined (bottom) MA 2

The Mg-Al HTlcs calcined at 750°C and 900°C were also characterized using FTIR. The IR spectra of the calcined materials are illustrated in Figure 4.11 and 4.12. It can be seen from the figures that for Mg-Al HTlcs calcined at 750°C and 900°C for all molar ratios, the broadband at 3700-2750cm^{-1} attributable to vibration of physically absorbed water, structural OH$^-$, vibrations of OH-OH, CO_3^{2-}-OH$^-$ and Mg^{2+}-OH$^-$ bonds of the hydrotalcite. All calcined samples exhibits bands at around 1650 cm^{-1} and 1450 cm^{-1} corresponding to water and carbonate molecules. This indicates that the samples still contained water and CO_2 even when high calcination temperature is used.

Additionally, for Mg-Al HTlcs samples calcined at both 750°C and 900°C it can be seen that at low wavenumber range, the bands indicating metal oxide (M-O) vibrations are not present expect for the MgO band at around 830cm^{-1} for Mg-Al HTlcs with Mg/Al molar ratio of three. The results show that the hydrotalcite structure is destroyed when HTlcs are calcined at high temperature and is in the agreement with the results obtained through XRD. Therefore, further characterizations of the samples via FESEM-EDX and N_2 adsorptions are not conducted on these HTlcs as they are considered to be already degraded at high calcination temperatures.

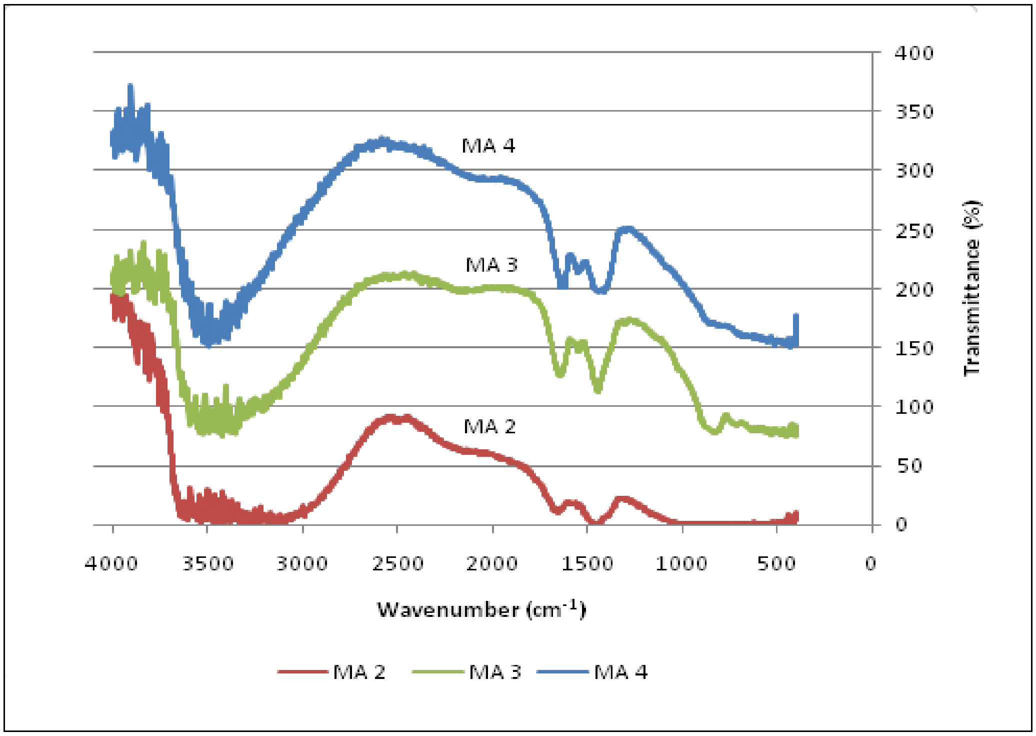

Figure 4.11: The IR spectra of Calcined Mg-Al HTlcs with Mg/Al molar ratio of 2 (bottom), 3 (middle) and 4 (top) calcined at 750°C

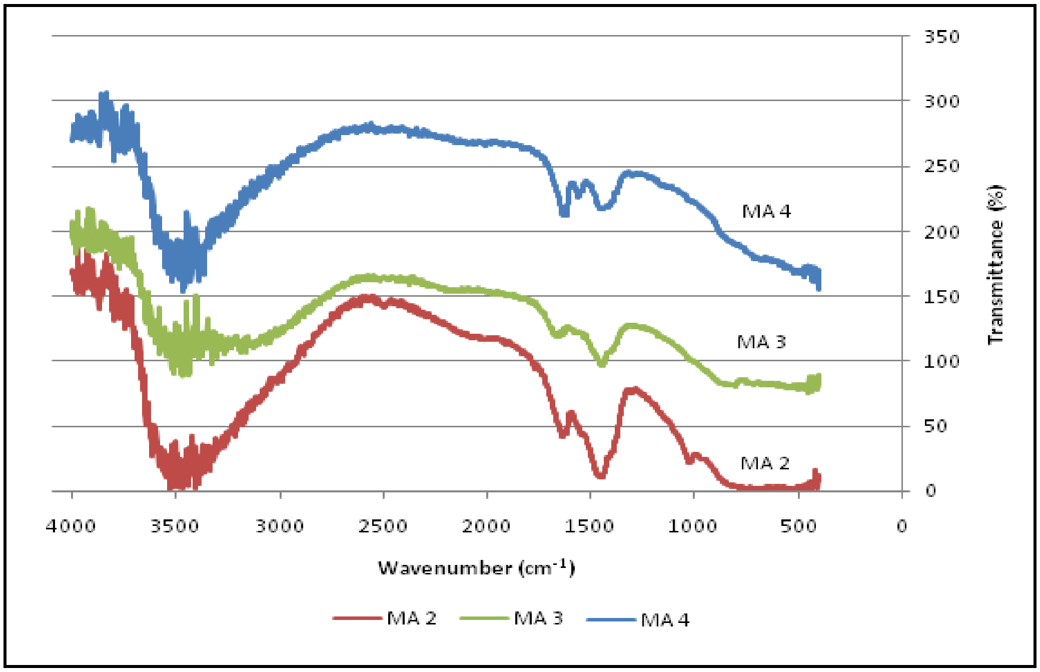

Figure 4.12: The IR spectra of Calcined Mg-Al HTlcs with Mg/Al molar ratio of 2 (bottom), 3 (middle) and 4 (top) calcined at 900°C

4.3.3. FTIR of As-Synthesized Ni-Mg-Al HTlcs

The Ni-containing HTlcs were also subjected to FTIR analysis and the IR spectra are shown in Figure 4.13. It can be seen that similar to the Mg-Al HTlcs, there is a main broadband in the range of 4000 and 2500cm^{-1} which can be attributed to the superimposition of vibrations due to physically adsorbed water, vibration of structural OH groups , vibrations of OH^{-} bonded to interlayer water and also interlayer carbonate ions. The bands at about 1633cm^{-1} for both samples are due to the adsorption caused by interlayer water molecules. The bands at 1372cm^{-1}and 1382cm^{-1} for the two samples show the vibration of carbonate species [18], [124]. The band for CO_3^{2-} vibration experienced splitting due to the lowering in the local symmetry of the carbonate anion in the interlayer space which arises from the interaction of the carbonate ions and water molecules in the hydrotalcite structure [74], [124].

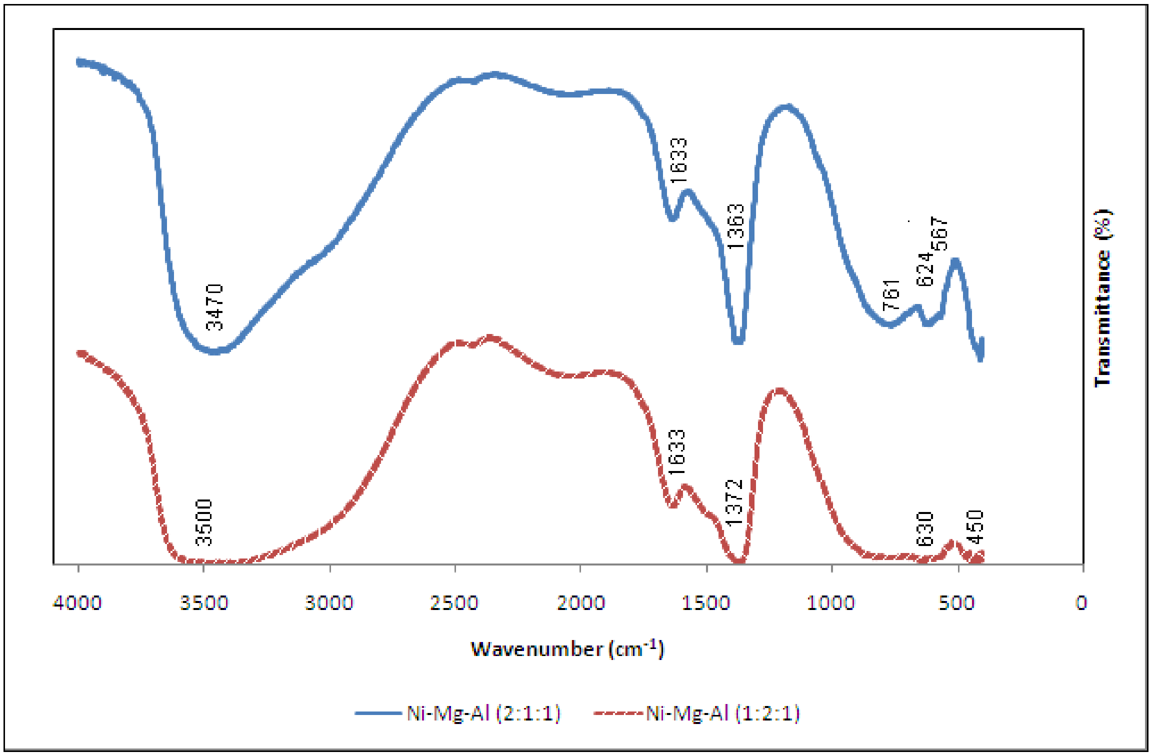

Figure 4.13: The IR spectra of as-synthesized Ni-Mg-Al HTlcs with Ni/Mg/Al molar ratio of 1:2:1 (bottom) and 2:1:1 (top)

Additionally, the bands recorded in the lower wavenumber range of 1000-400cm^{-1} are due to lattice vibrations involving layer cations [111]. For instance, the band at about 630 and 624cm^{-1} is due to the Mg-OH translations of the as-synthesized Ni-Mg-Al HTlcs with Ni/Mg/Al molar ratio of 1:2:1 and 2:1:1 respectively. Additionally, a band at 600 cm^{-1} can be assigned to Ni-OH translation but in the Ni-Mg-Al HTlc samples, it only appears as a shoulder around this value due to the lower nickel content compared to Ni-Al HTlcs, and this band of course is absent in Mg-Al HTlcs. Meanwhile, the Al-OH translation is indicated by the band present at 761 and 567cm^{-1} for Ni-Mg-Al HTlcs with Ni/Mg/Al molar ratio of 2:1:1 [74], [105].

4.3.4. FTIR of Calcined Ni-Mg-Al HTlc

The Ni-Mg-Al HTlcs samples with Ni/Mg/Al molar ratio of 1:2:1 calcined at 450 and 600°C were also subjected to FTIR analysis and the IR spectra are presented in Figure 4.14. Both Ni-Mg-Al HTlcs calcined at temperature of 450 and 600°C gives similar IR spectra shape but with different intensity. It can be seen from Figure 4.14 that Ni-Mg-Al HTlcs 1:2:1 calcined at 600°C gives lower intensity for water, hydroxyl and carbonate bands compared to the sample calcined at 450°.

Figure 4.15 shows the IR spectra of the as-synthesized and also calcined Ni-Mg-Al HTlcs samples. As illustrated in Figure 4.15, it can be seen that the shoulder at about 3100-3000cm^{-1} for bridging of H_2O-CO_3^{2-} has disappeared suggesting that elimination of water form the interlayer space occurred during calcination. However, there is still some water present in the material due to existence of the band ascribable to water at around 1600cm^{-1}. There is not much difference between IR spectra of as-synthesized and calcined samples for all Ni/Mg/Al molar ratios used indicating presence of hydrotalcite structure.

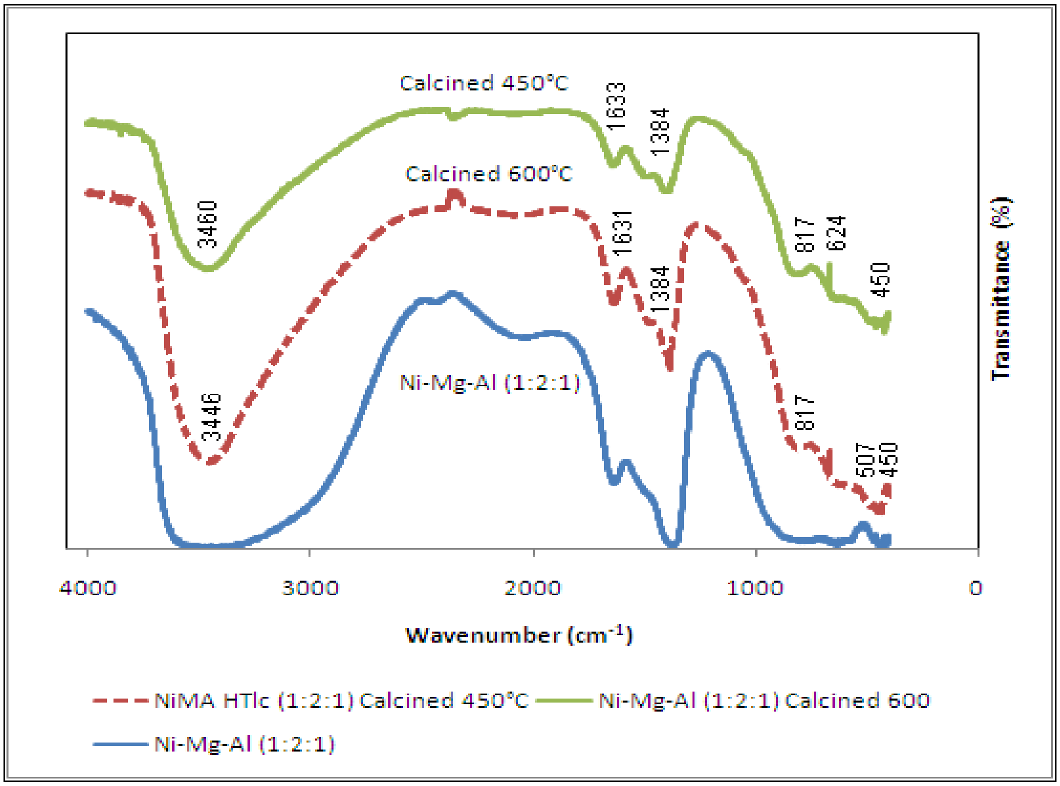

Figure 4.14: IR spectra of Ni-Mg-Al HTlc (1:2:1) calcined at 450°C and 600°C

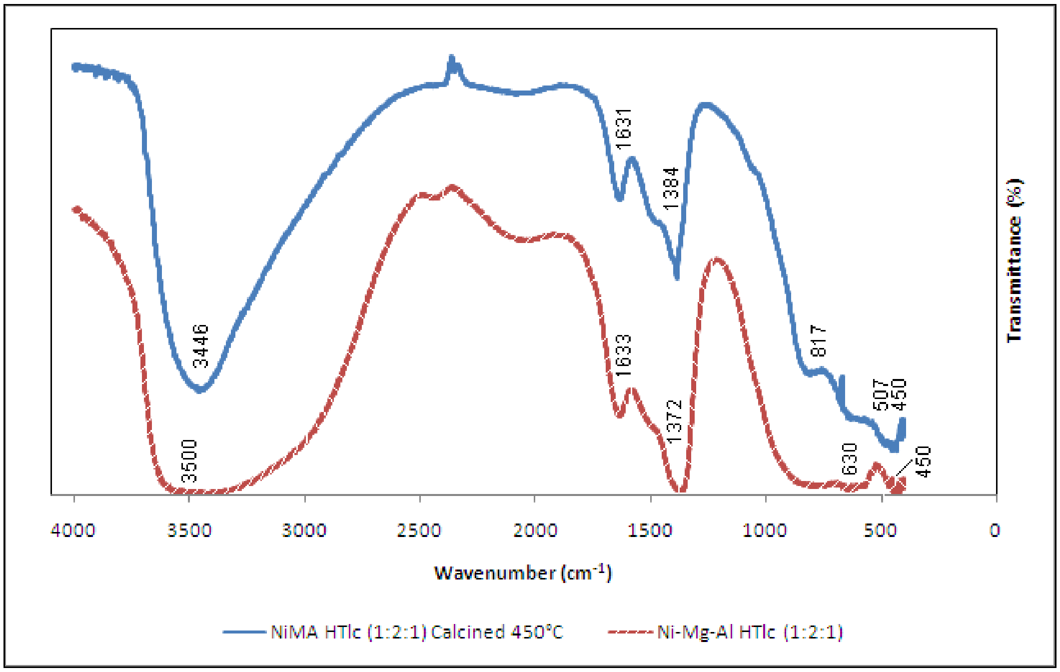

Figure 4.15: IR spectra of as-synthesized Ni-Mg-Al HTlc (1:2:1) (bottom) and Ni-Mg-Al HTlc (1:2:1) calcined at 450°C (top)

From the results of the FTIR and XRD analysis, it can seen that the hydrotalcite structure is retained even after calcination which is due to the memory effect. The memory effect is an important characteristic of HTlcs where the calcined material can be reformed into the hydrotalcite structure upon treatment with water and anions [142], [143]. Therefore it can also be said that the hydrotalcite structure of calcined HTlcs can be recovered in humid atmosphere and also aqueous solutions [17], [105]. However, as can be seen from the XRD results, the calcined HTlcs are less crystalline than the original samples indicating that the rehydration process is not entirely reversible [69], [144]. Furthermore, in previous work rehydration was found to occur only when the calcination temperature is below 600°C (873K) since higher temperatures prevented rehydration due to extensive spinel and oxide formation [69].

4.4. BET Specific Surface Area and Porosity Results

Adsorption of gases on a solid adsorbent is mainly related to the surface area and porosity of the adsorbent. The high surface area of adsorbents is desirable as it generally gives high number of adsorption-desorption sites. In order to study the surface area and porosity of synthesized materials, N_2 adsorption-desorption studies were conducted on the samples. The textural properties of the materials are presented in Table 4.1.

As shown in Table 4.1, the specific surface area of the samples increases for both uncalcined and calcined Mg-Al HTlcs when the Mg/Al molar ratio is increased from two to three in agreement with the result in a previous study [18]. The pore volume of Mg/Al HTlcs also generally increased with Mg/Al ratio and calcination step. However, the surface area of Mg-Al HTlc with molar ratio of two decreased with calcinations step due to collapse of the hydrotalcite structure as evident by XRD and FTIR. It can also be observed that when the Mg-Al HTlc with Mg/Al molar ratio of 3 is calcined at 450°C for three hours, the specific surface area increases nearly twice. This result is in agreement with previous investigations [17], [93], [104].

Table 4.1: Textural Properties of the Synthesized Hydrotalcites

Material	**BET Surface Area (m^2/g)**	**Pore Volume (cm^3/g) [BJH Desorption Cumulative Volume]**	**Pore Size (Å) [BJH Desorption average pore width (4V/A)]**
Mg-Al HTlc (Mg/Al = 2)	56.1680 m^2/g	0.155 cm^3/g	74.090 Å
Mg-Al HTlc (Mg/Al =3)	78.2383 m^2/g	0.268 cm^3/g	102.764 Å
Calcined Mg-Al HTlc (Mg/Al = 2) - 450°C	44.2673 m^2/g	0.236 cm^3/g	126.107 Å
Calcined Mg-Al HTlc (Mg/Al = 3) - 450°C	145.7959 m^2/g	0.400 cm^3/g	109.153 Å
Calcined Mg-Al HTlc (Mg/Al = 3) - 600°C	62.7790 m^2/g	0.230 cm^3/g	139.274 Å
Ni-Mg-Al HTlc (Ni:Mg:Al = 1:2:1)	152.0886 m^2/g	0.513 cm^3/g	105.431 Å
Ni-Mg-Al HTlc (Ni:Mg:Al = 2:1:1)	150.4930 m^2/g	0.387 cm^3/g	85.377 Å

The result observed is in agreement with the findings that with calcination at intermediate temperatures without losing the hydrotalcite structure, the surface area and pore volume increases. This is due to the formation of micropores and mesopores in the sample caused by the removal of CO_2 and water during calcination without altering the crystal morphology of the samples [93], [124], [138].

However, when the calcination temperature is increased to 600°C, the specific surface areas generally decrease. This trend where the surface area initially increases at calcination temperature of 450°C and then decreases at higher calcination temperatures has been reported in previous studies. It was suggested that this behaviour is due to the crystallization of the spinel-like phases [124]. Additionally, Kustrowski et al. [19] and Labajos et al. [131] stated that the decrease in specific surface area of the material is the result of the sintering of the crystallites. Apart from decreasing the surface area, increment of the calcination temperature will also increase the pore size and decrease pore volume as can be seen from Table 4.1 for Mg-Al HTlc with Mg/Al molar ratio of three. The decrease in surface area and pore volume with increasing calcination temperature has also been associated with the crystallization of well defined species such as MgO and $MgAl_2O_4$ [17]. Additionally, it can be observed that the calcination temperature influences the surface area greater than the composition of the samples does [138]. Meanwhile, for Ni-Mg-Al HTlcs, the surface area, pore volume and pore size are not much affected by Ni content. However, both surface area and pore volume significantly higher compared to Mg-Al HTlcs.

The pore size of the materials was also measureable through the N_2 adsorption technique. As can be seen from Table 4.1, all samples are of mesopore size (20-500Å). The material with the highest pore size is Mg-Al HTlc with Mg/Al molar ratio of 3 calcined at 600°C with a pore size of 139.274 Å. The results of the nitrogen adsorption showed that all HTlc samples exhibit the type IV isotherm which is characteristic of mesoporous materials [46], [93], [133] (isotherms are presented in Appendix 2). This mesoporosity of the samples are indicated by the existence of the hysteresis loop in the adsorption isotherms [49].

4.5. Field Emission Scanning Electron Microscope (FESEM)

In order to determine the morphology of the HTlcs, they were analyzed using field emission scanning electron microscope (FESEM). Additionally, the elemental compositions were determined using energy dispersive X-ray (EDX). Figure 4.16 and Figure 4.17 shows the FESEM images of Mg-Al HTlcs with Mg/Al molar ratio of two and three respectively. The HTlcs can be said to have coral-like morphology which agreed with previous investigations [108] – [110]. This morphology is observed as platelet pack to form quite open networks which indicate that the materials are porous in nature [93]. Meanwhile Figure 4.18 shows the FESEM image of the calcined Mg-Al HTlcs with Mg/Al molar ratio of three. There is not much change compared to the as-synthesized samples, however the pores of the materials is observed to be more visible after calcinations probably due to the removal of interlayer water and also carbonate ions.

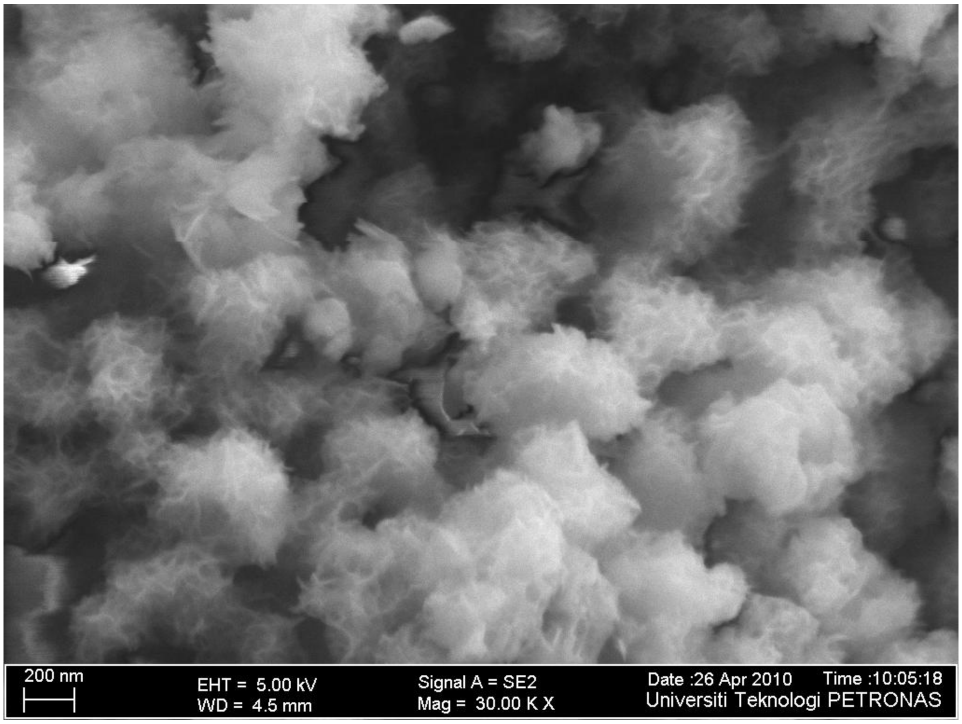

Figure 4.16: FESEM image for Mg-Al HTlc with Mg/Al molar ratio of 2

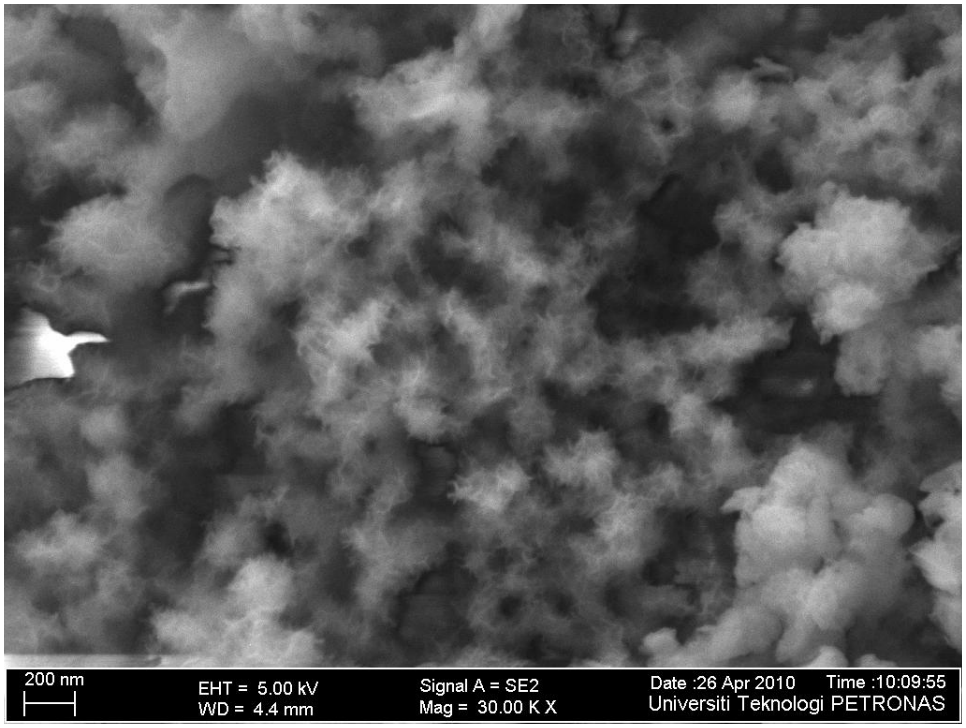

Figure 4.17: FESEM image for Mg-Al HTlc with Mg/Al molar ratio of 3

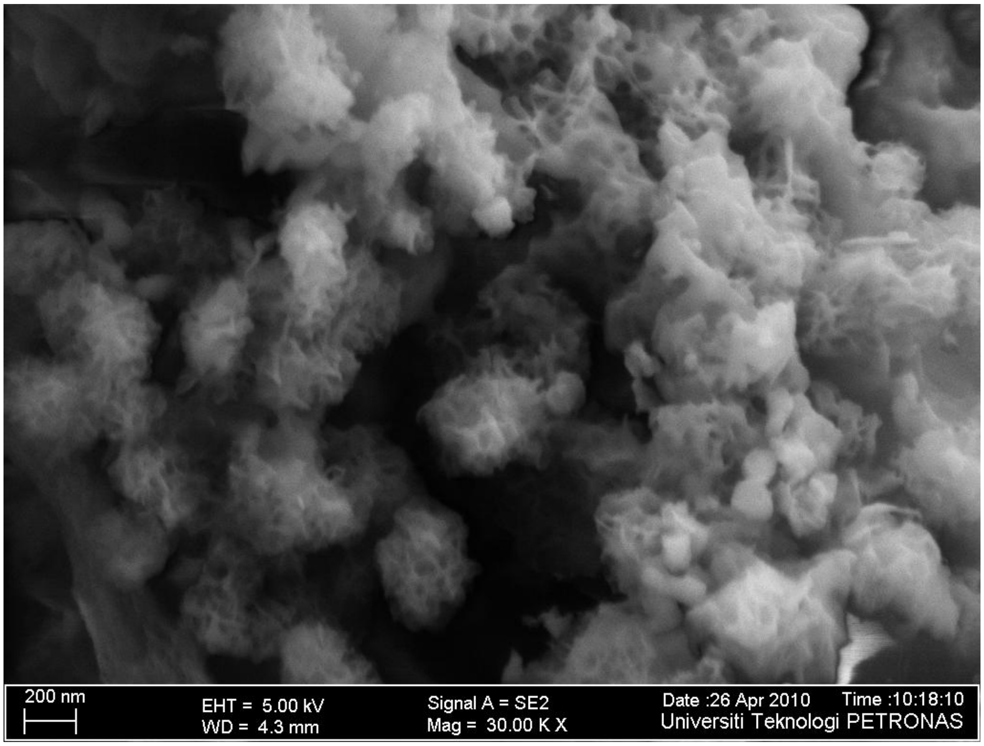

Figure 4.18: FESEM image for Mg-Al HTlc with Mg/Al molar ratio of 3 calcined at 450°C

Analysis of the selected Ni-Mg-Al HTlcs were also conducted using field emission scanning electron microscope-energy dispersive X-ray (FESEM-EDX). Figure 4.19 shows the FESEM images of Ni-Mg-Al HTlcs with Ni/Mg/Al molar ratio of 1:2:1. Meanwhile, Figure 4.20 shows the FESEM image for Ni-Mg-Al HTlcs with Ni/Mg/Al molar ratio of 2:1:1. It can be seen from both figures that the HTlcs consists of agglomerates of thin plate-like crystals which indicate layered structure and they also display the coral-like morphology that was observed for the previous HTlcs samples [110]. This indicates that the Ni-Mg-Al HTlcs also consists of porous layer structure. Additionally, calcined Ni-Mg-Al HTlcs with Ni:Mg:Al molar ratio of 2:1:1 were also analyzed using FESEM. The FESEM images are shown in Fig. 4.21 and 4.22. It can be observed from the FESEM image that the calcined Ni-Mg-Al HTlcs exhibits a similar morphology to the as-synthesized samples.

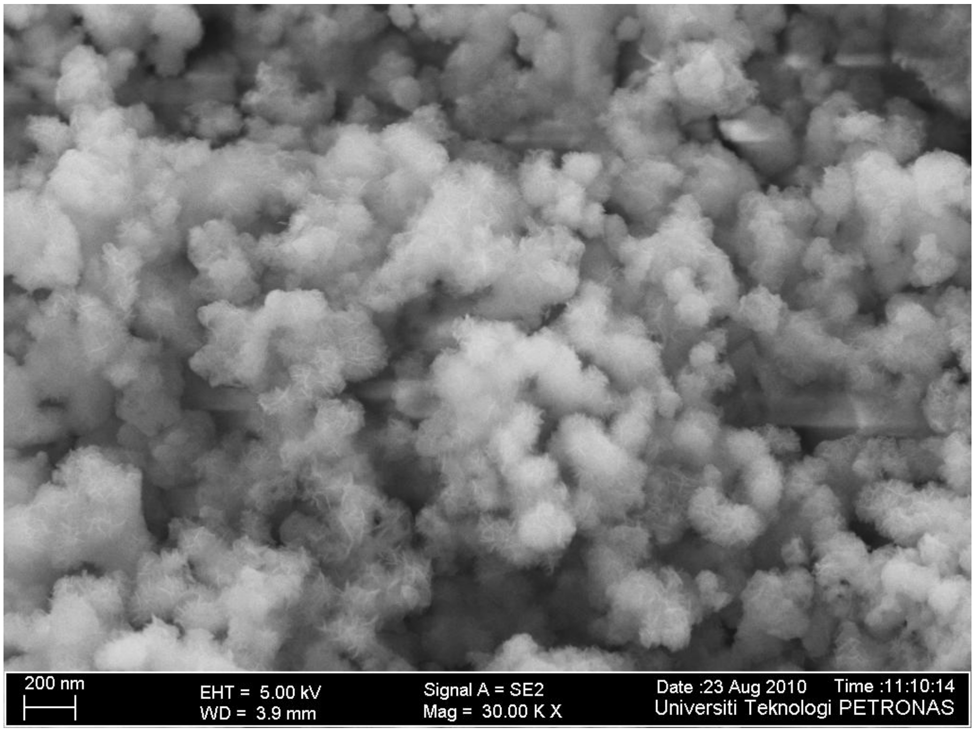

Figure 4.19: FESEM image of Ni-Mg-Al HTlcs with Ni/Mg/Al molar ratio of (1:2:1)

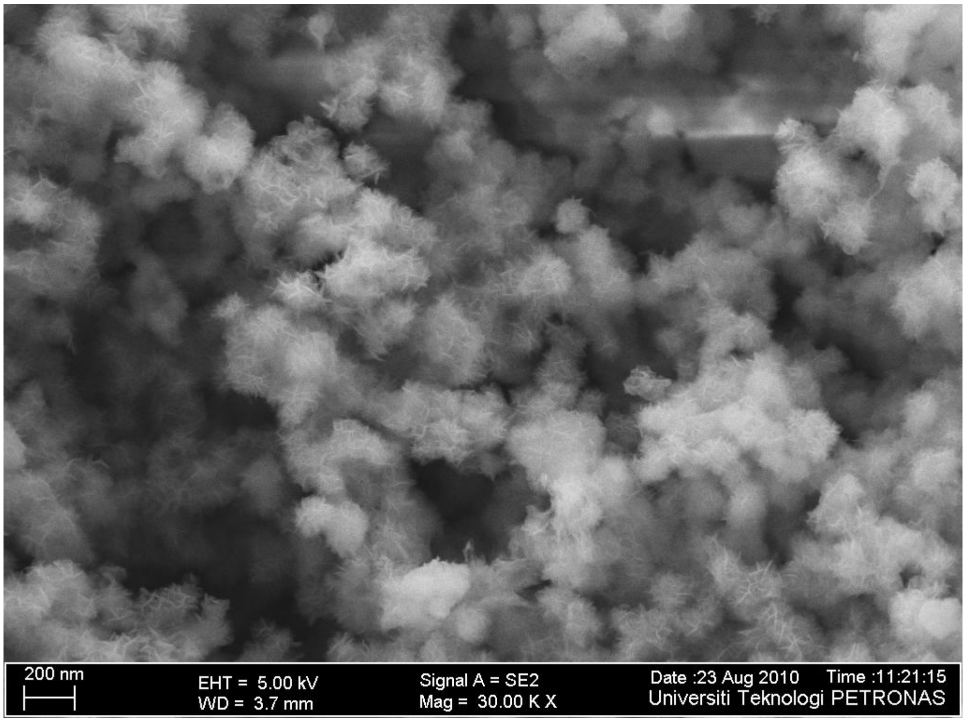

Figure 4.20: FESEM image of Ni-Mg-Al HTlcs with Ni/Mg/Al molar ratio (2:1:1)

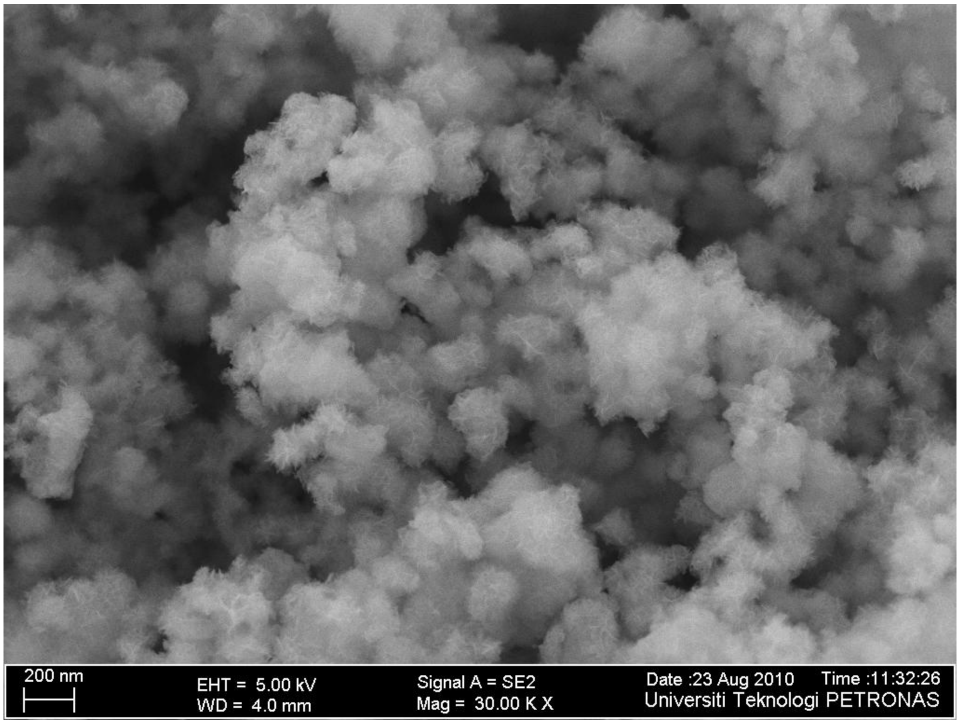

Figure 4.21: FESEM image of Ni-Mg-Al HTlcs (2:1:1) calcined at 450°C

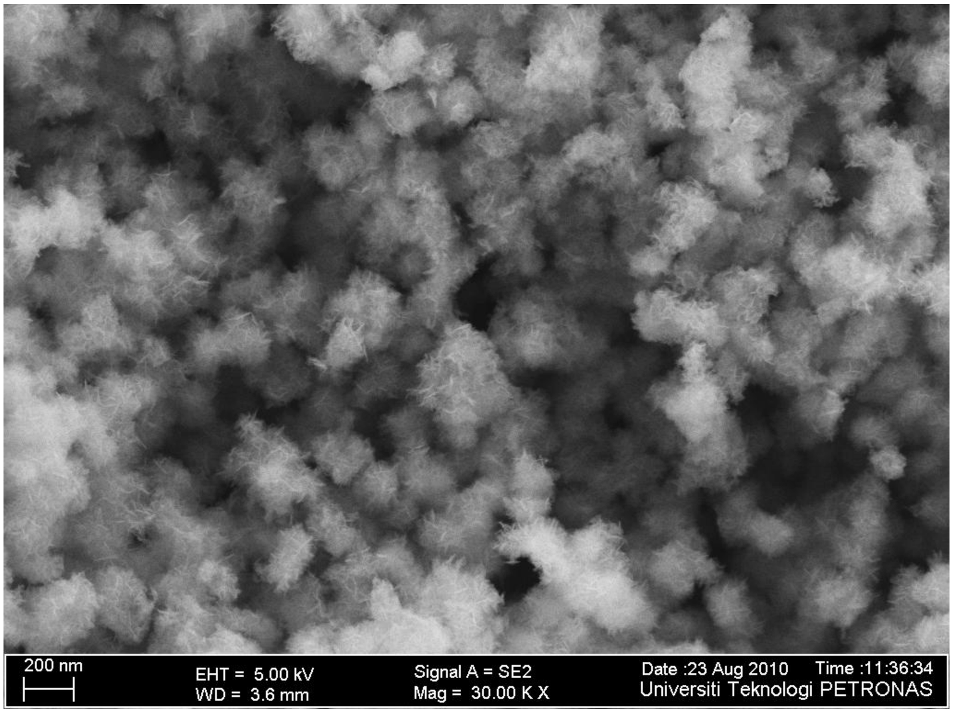

Figure 4.22: The FESEM image of Ni-Mg-Al HTlcs (2:1:1) calcined at 600°C

4.6. Energy Dispersive X-ray (EDX) Results

Chemical compositions of some of the materials as determined by energy dispersive X-ray, EDX analysis are presented in Table 4.2. For Mg-Al HTlc with nominal molar ratio three, the actual molar ratio was lower by about half. Meanwhile, for the Ni-Mg-Al HTlcs the measured molar ratios are close to the nominal. The difference between the M^{2+}/M^{3+} of starting solution and final synthesized material may be ascribed to a preferential precipitation of either one cation as hydroxide [107]. It seemed that more Mg-species was precipitated in the presence of Ni. It is also apparent that the carbon contents of the materials are high for Mg-Al HTlcs with molar ratio three. As shown in Table 4.2, the carbon contents are 26.17wt% for the as-synthesized HTlcs and 17.99wt% for the calcined Mg-Al HTlcs. The high carbon content may be due to remaining $NaCO_3$ in the samples [139].

Table 4.2: Chemical Composition of Hydrotalcite-like Compounds from EDX Analysis

Sample	**Molar Ratio**	**Actual Molar Ratio**	**Chemical composition (wt %)**					
			Mg	**Al**	**O**	**C**	**Na**	**Ni**
MA-3*	3	1.12	7.66	7.61	56.75	26.17	1.80	-
MA-3-600*	3	1.06	9.89	10.37	59.44	17.99	2.31	-
NiMA- 1:2:1#	1:2:1	1:1.7:1.3	10.13	8.82	58.39	7.81	-	14.85
NiMA-2:1:1#	2:1:1	2.2:0.7:1.1	3.73	6.34	51.65	12.22	-	26.07
NiMA-2:1:1-450#	2:1:1	2.2:0.6:1.2	5.06	12.11	38.26	-	-	44.58
NiMA-2:1:1- 600#	2:1:1	2.2:0.6:1.2	6.01	11.71	37.11	-	-	45.18

[*] Mg-Al HTlcs is designated as MA while the number following the hyphen is the Mg/Al molar ratio and the number after the second hyphen is the calcination temperature (°C)

[#] Ni-Mg-Al HTlcs are designated as NiMA while the number following the hyphen is the Ni/MgAl molar ratio and the number after the second hyphen is the calcination temperature (°C)

For Ni-Mg-Al HTlcs, the carbon contents are initially high but after calcination carbon cannot be detected in the samples. This may be because the carbon was totally released as carbon dioxide during the calcination stage. It can also be observed from the EDX results that the carbon content of Ni-Mg-Al HTlcs with Ni/Mg/Al molar ratio of 2:1:1 is higher than the one with 1:2:1 molar ratio. Additionally, Na content also cannot be detected since they have already been washed off during the synthesis step and only an undetectable amount is still present in the samples. Furthermore, it can been seen that increment of the calcination temperature does not significantly change the composition of the calcined products as can be seen in Table 4.2 for calcined Ni-Mg-Al HTlcs with Ni/Mg/Al molar ratio of 2:1:1. Again, the oxygen content of calcined Ni-Mg-Al samples is higher than theoretical by about 27%. This is due to remnants of amorphous hydroxyl groups that cannot be detected by XRD but evidenced by FTIR.

4.7. Temperature-Programmed Reduction (TPR) Results

The materials were subjected to temperature-programmed reduction (TPR) in order to determine the reducibility of the material and also the potential for subsequent hydrogen adsorption-desorption [123]. The materials were calcined in air at 450°C, 600°C, 750°C and 900°C for two hours in order to form mixed oxides and also to remove carbonate ions from the interlayer. During TPR experiments the samples were reduced under diluted hydrogen (5% H_2/95%N_2) flow and the temperature was increased from room temperature at a rate of 15°C /min.

4.7.1. TPR of Mg-Al HTlcs

Figures 4.23 to 4.26 illustrates the reduction profile for Mg-Al hydrotalcite-derived mixed oxides calcined at 450°C, 600°C, 750°C and 900°C respectively. The reduction profiles show a single reduction peak at reduction temperature of about 600°C for all the Mg-Al HTlcs. It can be seen from reduction profile in the figures that increasing the Mg/Al molar ratio generally decreases the amount of reduction of the Mg-Al HTlcs. However, for Mg-Al HTlcs calcined at 900°C, the reduction increases when the Mg/Al molar ratio is increased from two to three, and the amount of reduction then decreases when the Mg/Al molar ratio is further increased to four.

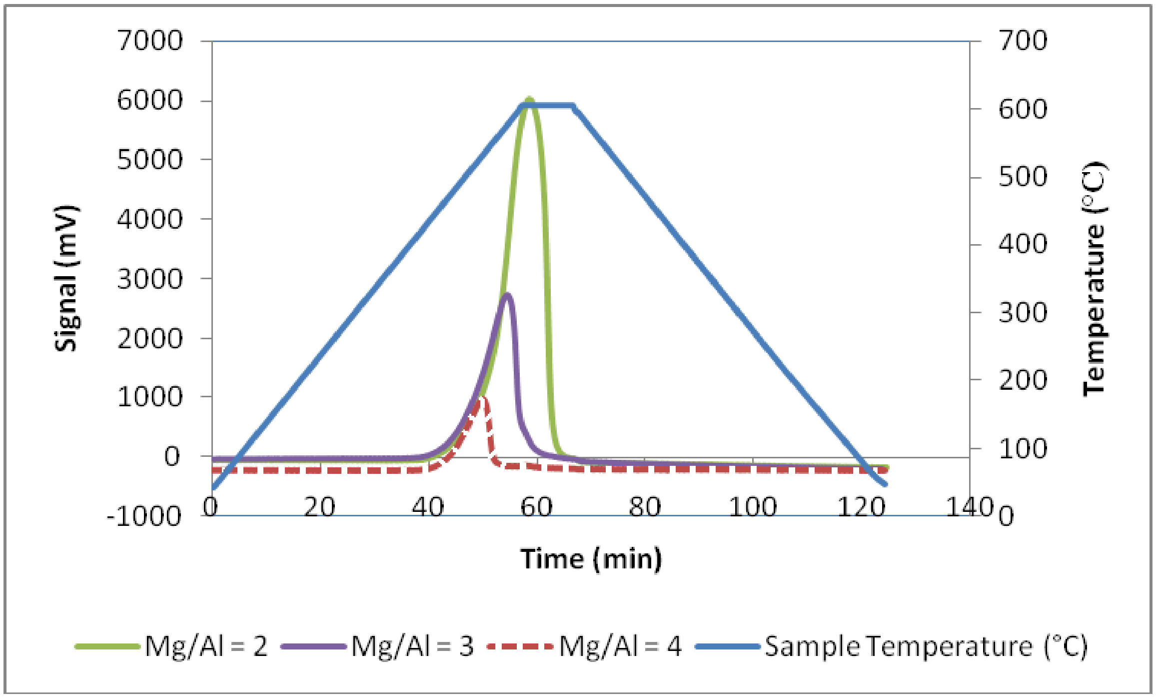

Figure 4.23 : Reduction profile for Mg-Al HTlcs calcined at 450°C

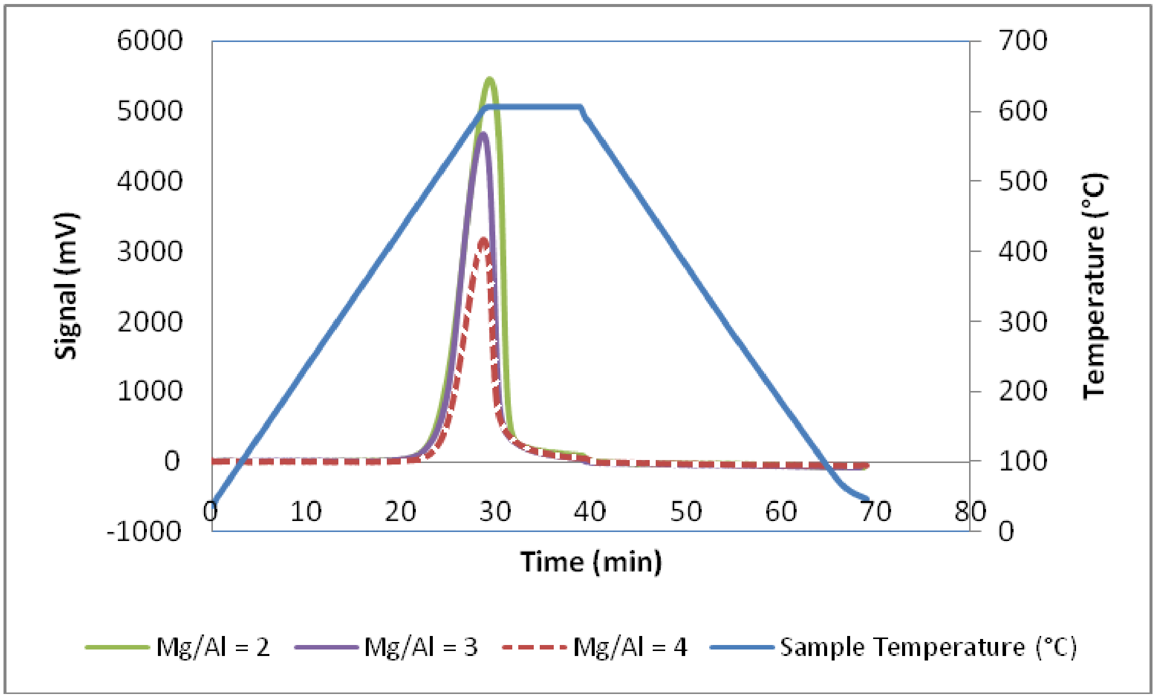

Figure 4.24 : Reduction profile for Mg-Al HTlcs calcined at 600°C

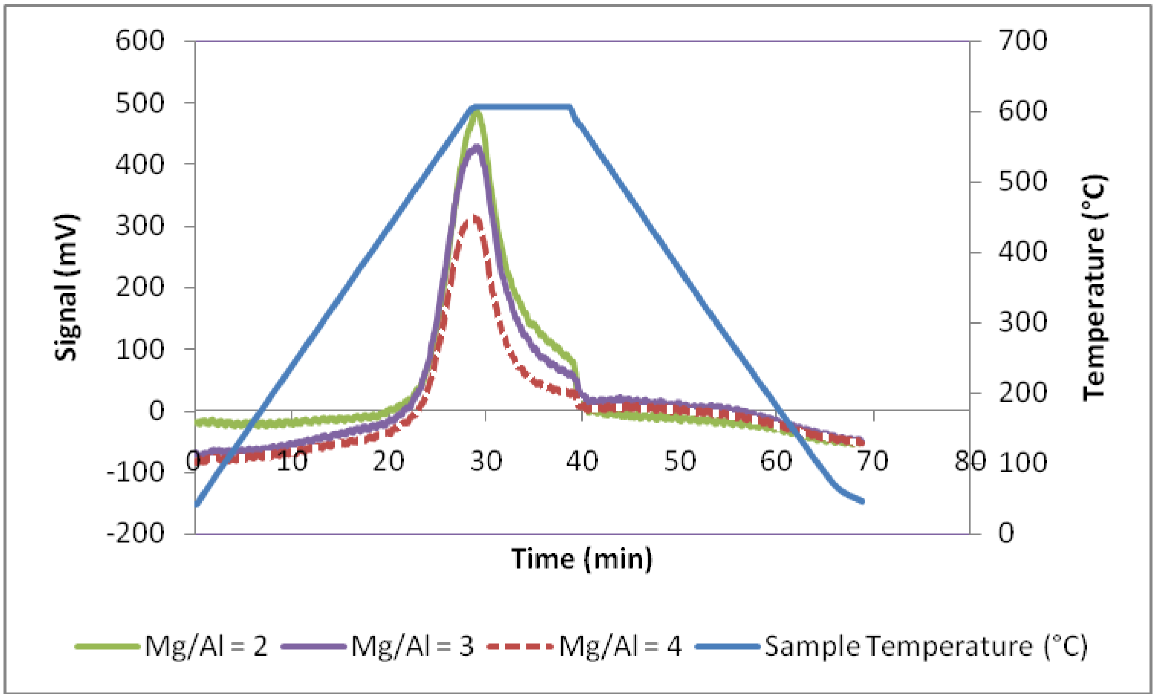

Figure 4.25 : Reduction profile for Mg-Al HTlcs calcined at 750°C

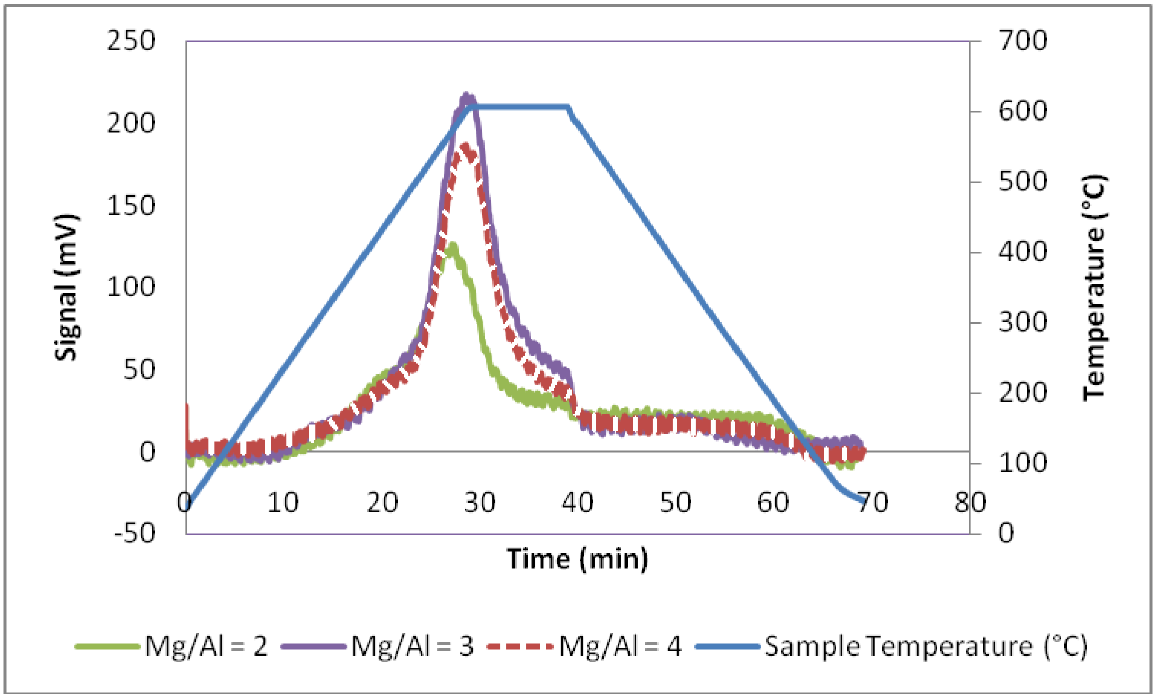

Figure 4.26 : Reduction profile for Mg-Al HTlcs calcined at 900°C

Subsequent to the TPR experiments, the reduced hydrotalcite-derived mixed Mg-Al oxides were subjected to X-ray diffraction in order to determine any structural changes that occurred upon reduction. The XRD profile for the reduced hydrotalcite-derived mixed Mg-Al oxides (calcination temperature 600°C) is shown in Figure 4.27. According to Figure 4.27, the hydrotalcite structure is still preserved in the reduced hydrotalcite-derived mixed oxides although not well crystallized. Additionally, the peaks at 2θ values of 18°, 20°, 61° and 64° can be attributed to hydrotalcite-like compounds. Figure 4.27 also show that MgO peaks at 38°, 43° and 62° are present indicating that MgO still exists in the sample. This implies that only a small amount of MgO oxide was reduced during TPR experiments. However, detection of metals or metal hydride by XRD is traditionally difficult. Other reduced samples tested using XRD showed similar pattern as the one in Figure 4.27 indicating presence of hydrotalcite phase even after reduction process.

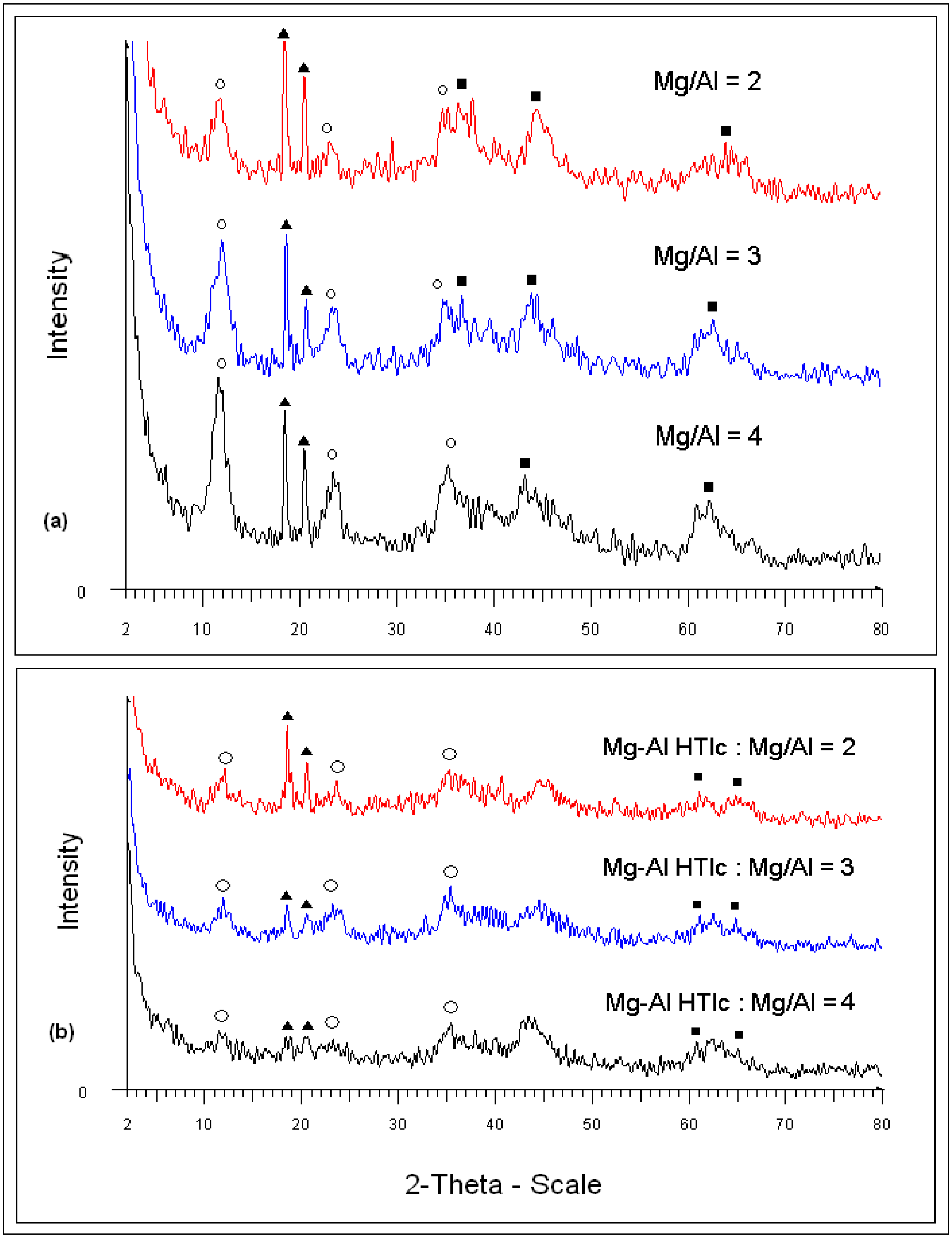

Figure 4.27: XRD pattern for Mg-Al HTlcs calcined at 600°C (a) before reduction and (b) after reduction: ○ Hydrotalcite, ■ MgO, ▲ Gibbsite

4.7.2. TPR of Ni-Mg-Al HTlcs

The reduction profiles obtained when as-synthesized Ni-Mg-Al HTlcs were analyzed using temperature programmed reduction (TPR) are presented in Figure 4.28 and Figure 4.29. TPR was carried out on the as-synthesized Ni-Mg-Al HTlcs samples to determine their reducibility and also possible hydrogen uptake.

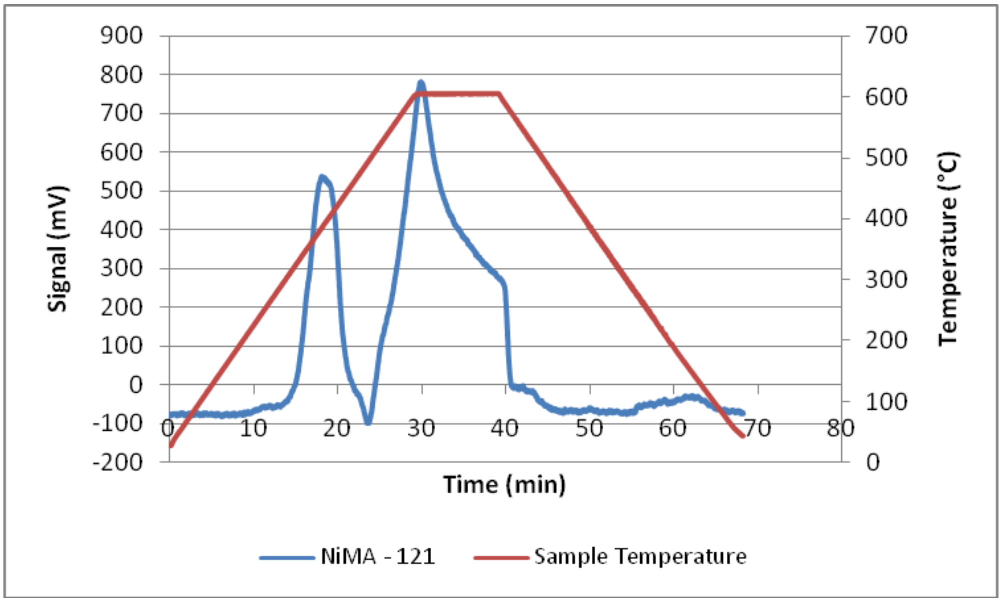

Figure 4.28: Reduction profile of as-synthesized Ni-Mg-Al HTlcs (1:2:1)

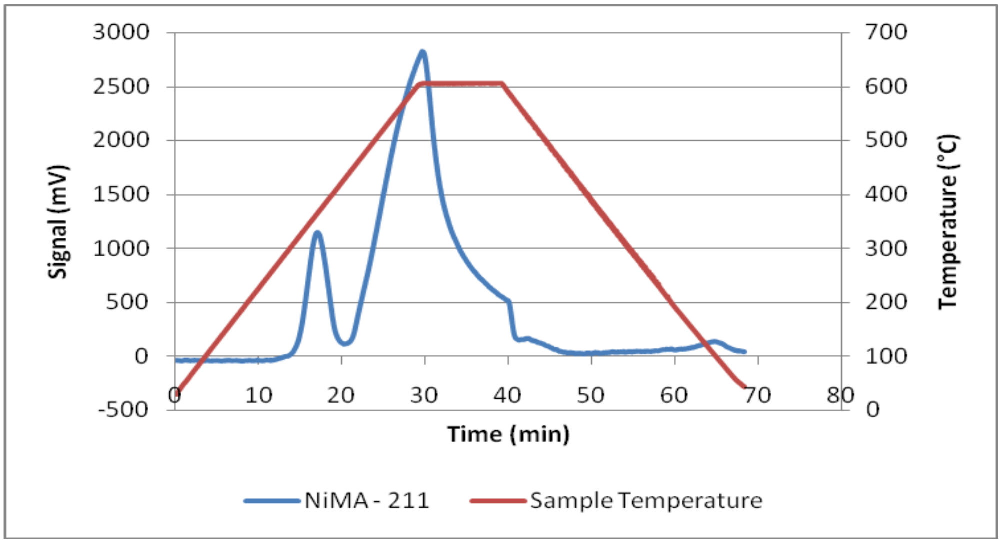

Figure 4.29: Reduction profile of as-synthesized Ni-Mg-Al HTlcs (2:1:1)

Referring to Figure 4.28 and Figure 4.29, it can be seen that for both as-synthesized Ni-Mg-Al HTlcs samples there are two reduction peaks at about 400°C and 600°C respectively. The result is in agreement with the study by Rives et al., [145] where the TPR of Ni-containing HTlcs also produced two reduction peaks. The reduction of unsupported NiO is known to display a single reduction peak at approximately 367°C (in the range of 250-427°C) [27] [146]. The presence of two separate peaks in Ni-containing HTlcs is also observed.

The results are also comparable with the findings of Kawabata et al. [73], where two reduction peaks at 300°C (773K) and 500°C (623K) were observable for the TPR of nickel-containing Mg-Al HTlcs. The first peak at around 400°C for both as-synthesized samples can be ascribed to the reduction of Ni^{2+} species from NiO present in the hydrotalcite layers [73], [145]. Thus, the first peak corresponds to the nickel oxide reduction since this peak is not present in the reduction profile of Mg-Al HTlcs. Meanwhile, the second peak at about 600°C is probably due to the reduction of the remaining Ni^{2+} in Ni(Al)O or periclase Mg(Ni,Al)O [73] and may possibly be a result of the subsequent hydrogen uptake by the reduced material as temperature is decreased as evidenced by tailings of the curves. It is stated that Mg(Ni,Al)O is present since the sample is considered to be dehydrated and decomposed into mixed oxides by 600°C [73].

It can also be seen from Figure 4.28 and Figure 4.29 that when the Mg content is increased in the as-synthesized Ni-Mg-Al HTlcs samples, the reduction peaks shifted towards higher temperature. The reduction peaks are at about 340°C and 590°C for Ni-Mg-Al HTlcs with Ni/Mg/Al molar ratio of 2:1:1 while the peaks are present at 400°C and 600°C for Ni-Mg-Al HTlcs with Ni/Mg/Al molar ratio of 1:2:1. The increasing Mg content also gives reduction peaks with lower intensities. It has been suggested that the higher reduction temperature for higher Mg content may be due to the stabilization of the Ni^{2+} that is incorporated in the periclase Mg(Al)O via the formation of solid solutions such as Mg(Ni,Al)O. Increasing the Mg/Ni ratio could also increase this stabilization effect [73]. In another study, it was stated that increasing the magnesium content in the Ni-Mg-Al HTlcs higher in excess of the stoichiometric amount, decreases the reducibility of the Ni since this results in the formation of MgO in addition to $MgAl_2O_4$. The Ni will react with the MgO forming NiO-MgO solid solution which is highly stable and hard to be reduced [128], [129].

Additionally, the calcined Ni-Mg-Al with molar ratio of 1:2:1 were also analyzed using TPR. The resulting reduction profiles are shown in Figure 4.30 and 4.31. It can be seen that for the Ni-Mg-Al HTlc calcined at 450°C, there are three reduction peaks, while as the calcination temperature is increased to 600°C only one reduction peak is visible. The two reduction peaks at 250°C and 400°C combines to give a single broad peak at 200-400°C. Only one reduction peak present in the samples calcined at higher temperatures may be due to the absence of isolated NiO in the sample [147] which may be because of the high calcination temperature used [73]. It has been previously observed that the reducibility of Ni-Mg-Al HTlc decreases with increase in Mg and Al content as well as the increase of calcination temperatures [112]. Again, tailings at 600°C and subsequent decreasing temperature indicate hydrogen adsorption on the reduced nickel oxide.

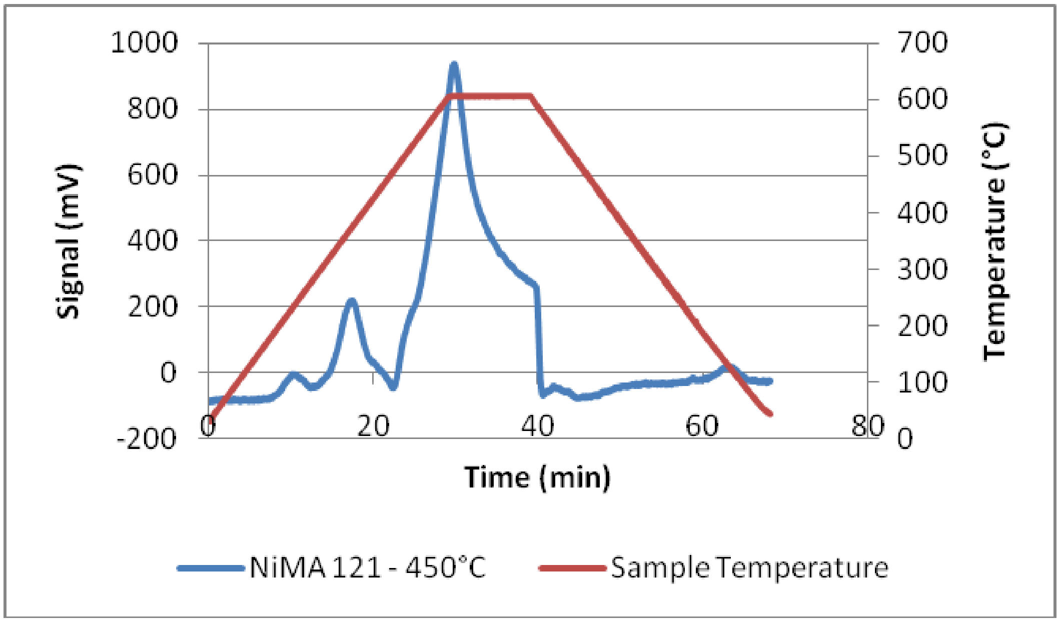

Figure 4.30: Reduction profile of Ni-Mg-Al HTlcs with Ni/Mg/Al ratio 1:2:1 calcined at 450°C

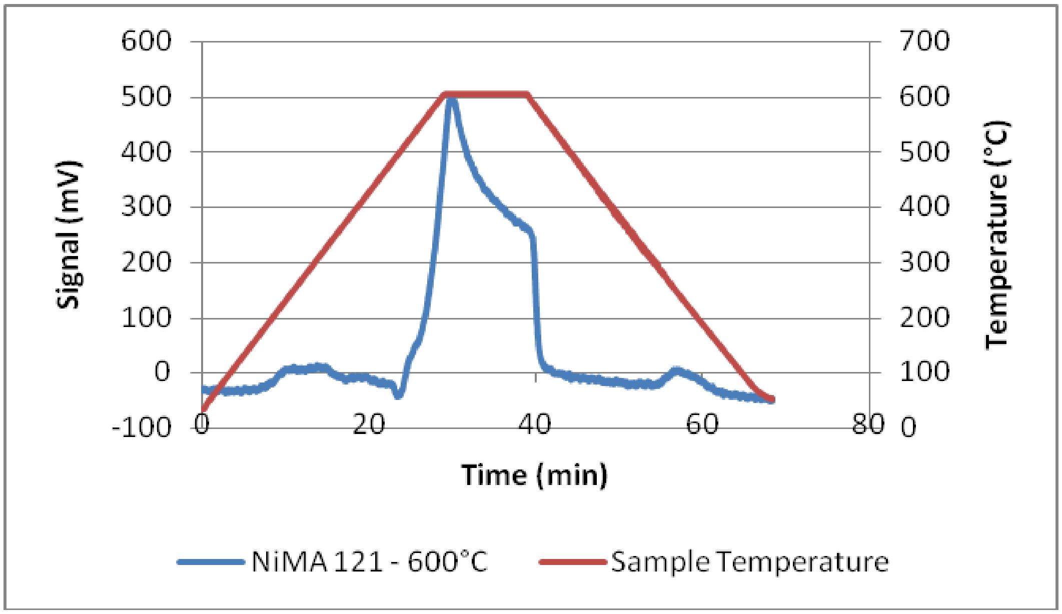

Figure 4.31: Reduction profile of Ni-Mg-Al HTlcs with Ni/Mg/Al ratio 1:2:1 calcined at 600°C

4.7.3. Hydrogen Consumption by the Materials during TPR

During the TPR experiments, the reduction process of the materials can be detected by the amounts of H_2 consumption. Figure 4.32 presents the hydrogen consumption of Mg-Al HTlcs calcined at different temperatures. In the figure, Mg-Al HTlcs is designated as MA and the following number is the Mg/Al molar ratio.

As illustrated in Figure 4.32, Mg-Al HTlcs with Mg/Al molar ratio two calcined at 450°C gives the highest hydrogen consumption of 3.176 mmol H_2/g. Second highest hydrogen consumption is also by Mg-Al HTlcs with Mg/Al molar ratio two calcined at 600°C which is 2.079 mmol H_2/g. Although the hydrogen consumptions of the materials are quite small, they are still comparable to results of a previous research [127], where the TPR of Mg^{2+}-Mn^{3+}-carbonate anionic clay, decavanadate-pillared hydrotalcite, and Ni^{2+}-Al^{3+}-carbonate anionic clay gave hydrogen consumptions of 1.1, 4.7 and 6.4 mmol H_2/g respectively. The small hydrogen consumption of the material maybe due to the low reducibility of Mg-Al hydrotalcite-derived mixed oxides [24], [127].

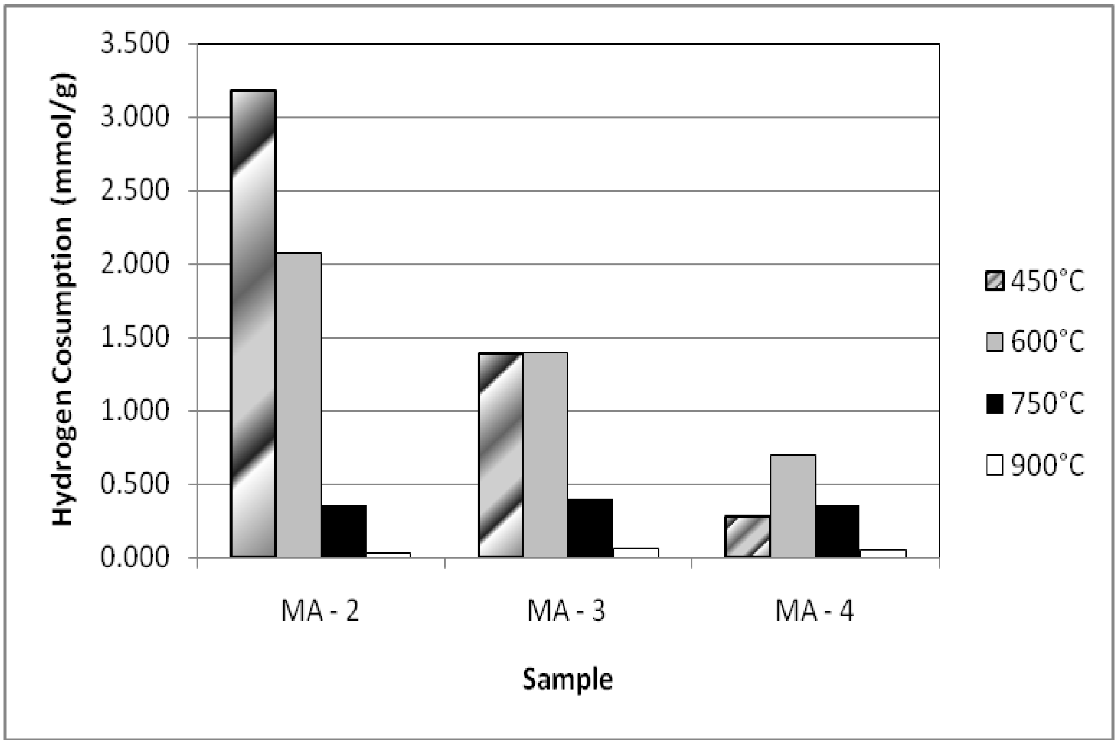

Figure 4.32: Hydrogen consumption of Mg-Al HTlcs during TPR

The reason for generally decreasing amount of reduction with increase in Mg/Al molar ratio may be that incomplete mixed oxide formation during calcination. It can be seen from Figure 4.32 that for a given sample, increasing the calcinations temperature generally decreases the amount of hydrogen consumption. It seemed that retention of the hydrotalcite structure is more favourable for hydrogen consumption than the formation of oxides which are unreducible. A small amount of reduction of oxides formed at higher calcinations temperatures (750-900°C) can be evidenced by tailing of the TPR curves. It may also be contributed to hydrogen spill-over effect on the mixed oxides formed. Further tailings at decreasing temperatures may indicate hydrogen adsorption.

The hydrogen uptake by Ni-Mg-Al HTlcs increased from 1.027mmol/g to 3.293mmol/g with increase in nickel content. This is because more reducible species is present in the sample with increase in nickel content. Additionally, it can be seen from Figure 4.33 that for Ni-Mg-Al HTlcs with Ni/Mg/Al molar ratio of 1:2:1, the hydrogen consumption during TPR are similar for the as-synthesized and also calcined samples.

The equally high hydrogen uptake by the calcined samples is due to the contribution of the hydrotalcite-like structure which provided adsorption sites for hydrogen.

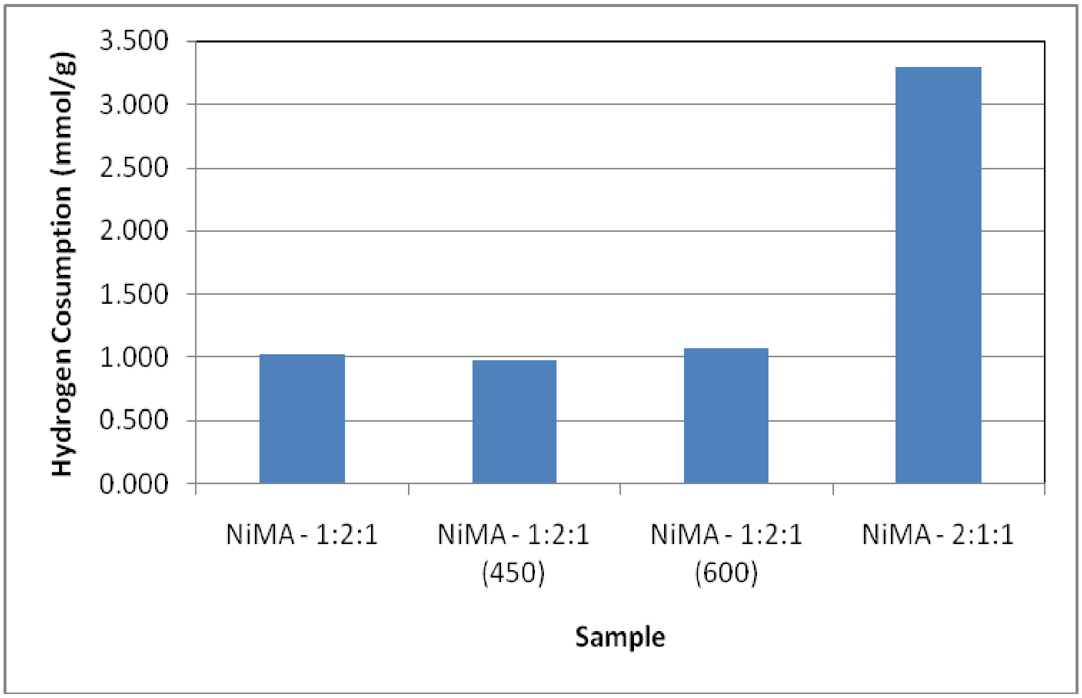

Figure 4.33: Hydrogen consumption of Ni-Mg-Al HTlcs during TPR

4.8. Thermogravimetric Analysis Results

The hydrogen adsorptions for the HTlcs and derived mixed oxides were studied using thermogravimetric analysis (TGA). The as-synthesized were subjected to TGA and the weight losses of the samples were recorded against time. The thermogravimetric (TG) curve for the selected HTlc sample is presented in Figure 4.34.

The TG curves for all the tested HTlc samples is similar to that of Mg-Al HTlc with molar ratio two, which is presented in Figure 4.34. According to the TG curves of the HTlcs, during the pre-treatment stage when they were heated up to 600°C under diluted hydrogen (5%H_2/95%N_2), all samples experienced a two stage weight loss. This result has also been recorded in previous research [76], [93].

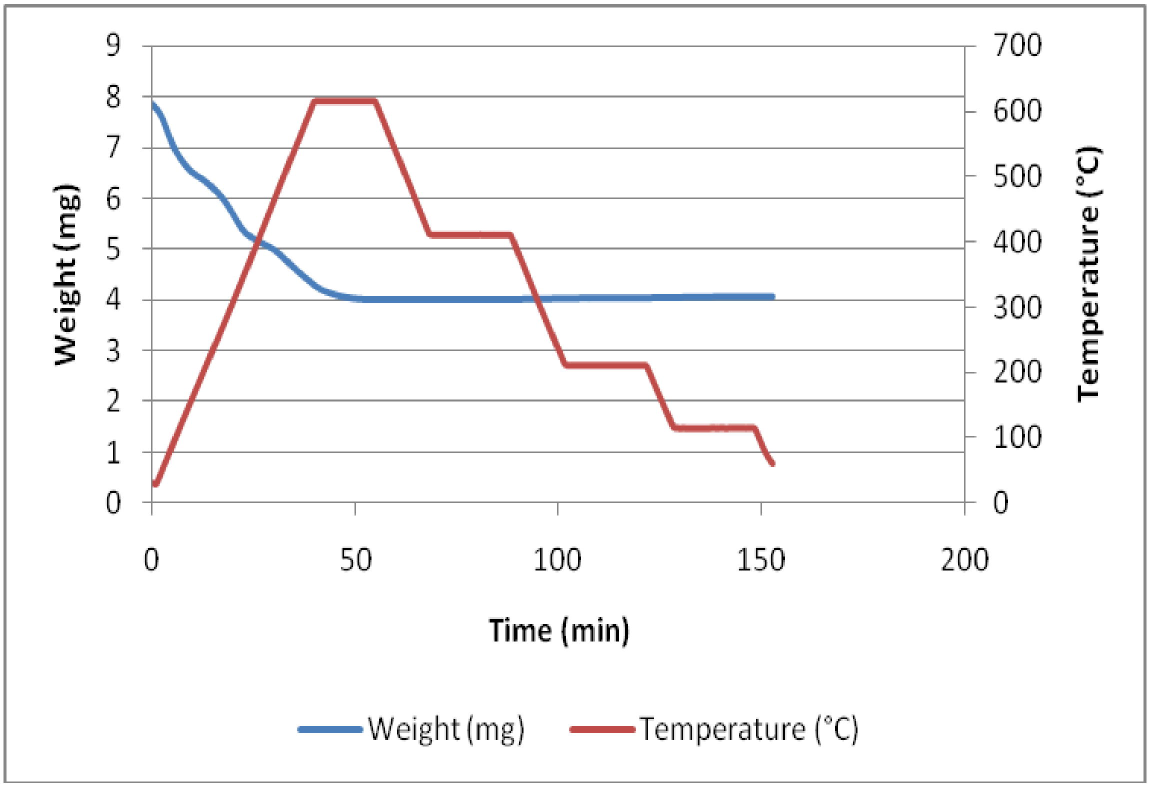

Figure 4.34: TG Curve of as-synthesized Mg-Al HTlc with Mg/Al molar ratio of 2

The first weight loss can be attributed to the removal of water molecules from the interlayer region while the second weight decrement is due to the simultaneous elimination of hydroxyls (as water) and carbonates (as CO_2) from the HTlcs [93], [111], [118]. The aim of this heating the sample to 600°C is to provide fresh adsorbent for the adsorption process. Additionally, it is also required to provide mixed oxides with HTlc skeletal structure for gas adsorption [95]. The two stage weight loss and formation of the mixed oxides form Ni-Mg-Al HTlcs can be presented as in the following formulas [111]:

For the first weight loss due to elimination of interlayer water,

$$[Mg_{1-x-y}Ni_yAl_x(OH)_2](CO_3)_{x/2}\cdot nH_2O \rightarrow [Mg_{1-x-y}Ni_yAl_x(OH_2)](CO_3)_{x/2} \tag{4.1}$$

The next formula is for the second weight loss and formation of mixed oxides

$$[Mg_{1-x-y}Ni_yAl_x(OH)_2](CO_3)_{x/2} \rightarrow [(1-x-y)MgO + yNiO + (x/2)Al_2O_3] + H_2O + (x/2)CO_2 \tag{4.2}$$

From equation 4.2, we can see that after the second weight loss, the HTlcs are changed into mixture of MgO, Al_2O_3 and NiO (only for Ni-Mg-Al HTlcs) [124]. The percentage of weight losses for the HTlcs during the pretreatment are shown in Table 4.3. It can be seen from the table that the weight decreases experienced by the samples are between 40 to 50 percent. Subsequently, the mixed oxides would be continuously exposed to diluted hydrogen in order to determine its potential as hydrogen storage adsorbent.

Table 4.3: The weight decrease of HTlcs samples after the pretreatment stage

Sample	Weight Decrease (wt%)
Mg-Al HTlc (Mg/Al = 2)	48.945
Mg-Al HTlc (Mg/Al = 3)	48.870
Mg-Al HTlc (Mg/Al = 4)	47.933
Ni-Mg-Al HTlc (Ni:Mg:Al = 1:2:1)	44.028
Ni-Mg-Al HTlc (Ni:Mg:Al = 2:1:1)	40.854

The weight decrease is also observed when the adsorbents are calcined in a furnace under inert conditions at a temperature of 450°C for three hours. The weights of the samples were reduced to about 40 percent of the initial weight before calcination. The resulting amounts were achieved since the decomposition of the HTlcs causes the removal of about 40 percent of the initial weight while about 15 percent of the total initial weights of carbonate-containing HTlcs consist of interlayer water. The remaining weight loss after the calcination of the HTlcs can be attributed to the removal of carbonate ion (as CO_2) and hydroxide ion (as water vapour) via decarbonation and dehydroxylation [17]. The TG curves for the second part of the experiment or the adsorption part when the system temperature is decreased is shown in Figure 4.35. The adsorption branch for the thermogravimetric curve is similar for all samples. It can be seen for all the HTlcs samples that there is a weight increase as the temperature is lowered.

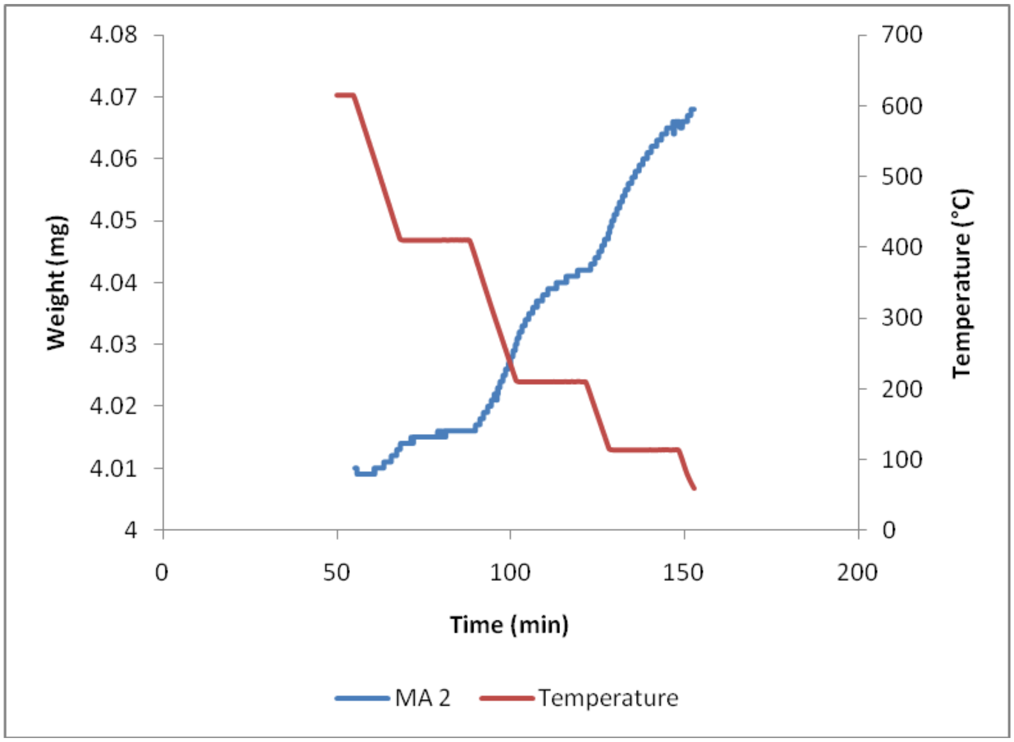

Figure 4.35: The adsorption branch of the TG Curve of as-synthesized Mg-Al HTlc with Mg/Al molar ratio of 2

The weight increase during the TG experiment can be taken as the hydrogen uptake by the reduced HTlcs. Additionally, the samples were kept at holding temperatures of 400°C, 200°C and 100°C to investigate the total adsorption capacity at these temperatures. The holding temperatures were applied in this study in order to allow the system to reach steady state where no appreciable change of mass occurred [122]. The weight increase of the Mg-Al HTlcs samples at each holding temperature decreased when the Mg/Al molar ratio was increased from two to three before increasing when the Mg/Al molar ratio was four. The smaller weight increase displayed by Mg-Al HTlc with Mg/Al molar ratio of three may be because of the decrease in surface area of the sample when it is heated to high temperature of 600°C as indicated by the BET surface area values.

From Figure 4.35 it can be seen that the HTlcs has most likely reached the equilibrium adsorption at high holding temperatures due to the horizontal line that can be observed in the figures. It can be said that a holding time of 20 minutes is quite sufficient for the HTlcs to reach equilibrium at high (>100°C) holding temperatures. However at 100°C, the equilibrium is still not reached after 20 minutes.

The weight increase of the samples after TGA as shown in Figure 4.36 shows that for all samples the adsorption capacities are reduced with increasing temperatures. This result indicates that high temperature leads to lower adsorption capacity. It showed that the adsorption capacity reflects the exothermicity of adsorption where the equilibrium adsorption capacity of a system, decreases with increasing temperature [43], [122].

As shown from Figure 4.36, it can be seen that Ni-Mg-Al HTlc with less nickel content gave higher amount of hydrogen adsorption which may be due to higher reducibility compared to the Ni-rich sample. The existence of a surface spinel-type phase may be the cause of the lower reducibility for the sample with higher Ni content since this reduces the access of the surface by the reducing gas mixture [138]. It can also be seen from Figure 4.36 that Ni-Mg-Al HTlc with Ni/Mg/Al molar ratio of 2:1:1generally gives the second highest hydrogen adsorption after Ni-Mg-Al HTlc with the lower nickel content. The results of TGA showed that Ni-Mg-Al HTlc with Ni/Mg/Al molar ratio of 1:2:1 gives the highest gas uptake of about 3.093wt% at 100°C. These results are due to better reducibility of Ni compared to the other metals. A previous research found that the addition of nickel into Mg-Al HTlc increased the reducibility of the HTlcs [145].

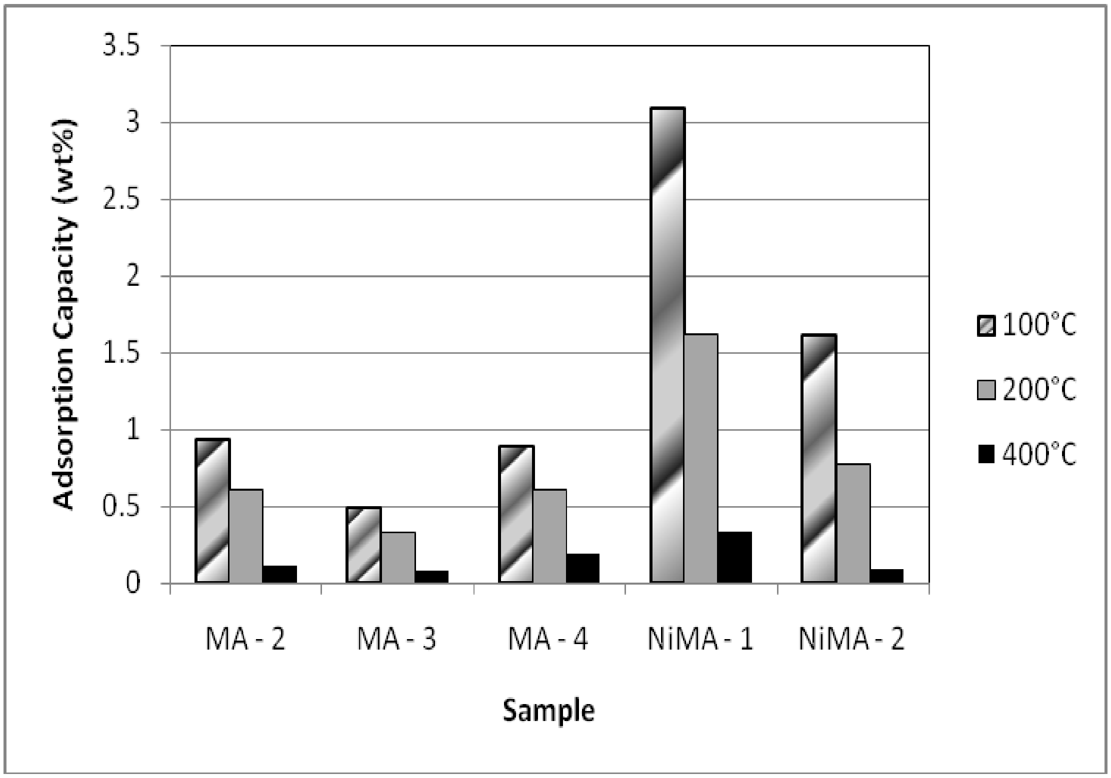

Figure 4.36: Hydrogen adsorption capacity of the HTlcs samples at various temperatures

It can be seen form the histogram in Figure 4.36 that the adsorption capacity for Ni-Mg-Al is comparable to that of Mg-$LaNi_5$ composite (3.8wt%) at 100°C [127].

Furthermore, the initial adsorption rates of the HTlcs can also be determined from the thermogravimetric results and they are shown in Table 4.4. The initial adsorption rates were calculated from the slope of the first weight increase at the holding temperature of 400°C.

The adsorption rate at constant temperature is calculated for initial adsorption that occurred during the first 10 minutes at holding temperature 400°C. This is because during this period, the temperature of the system is almost constant at this value. The adsorption rate may be calculated using the Linear Driving Force (1st order) model.

$$\frac{d\alpha}{dt} = k_O^{-\frac{E}{RT}}\left(1-\alpha\right) \tag{4.3}$$

Where α is the degree or fraction of adsorption:

$$\alpha = \frac{w - w_0}{w_f - w_0} \qquad (4.4)$$

For the adsorption rate between the temperatures of 400 and 200°C, w_0 is the weight at 400, w_f is the weight at 200°C and w is the weight at the first 10 minutes of adsorption where temperature is considered constant. Equation 4.3 can also be written in logarithmic form as in the following.

$$\ln\left|\frac{d\alpha}{dt}\right| = -\frac{E}{RT} + \ln\left[k_O(1-\alpha)\right] \qquad (4.5)$$

Then using equation 4.5 the graph of ln[dα/dt] versus 1/T can be plotted. The slope is –E/R, therefore from the slope the activation energy E can be obtained since R is the gas constant. On the other hand, the adsorption rate can be obtained from the slope of the plot of adsorption amount to the time of adsorption as shown in the example in Figure 4.37.

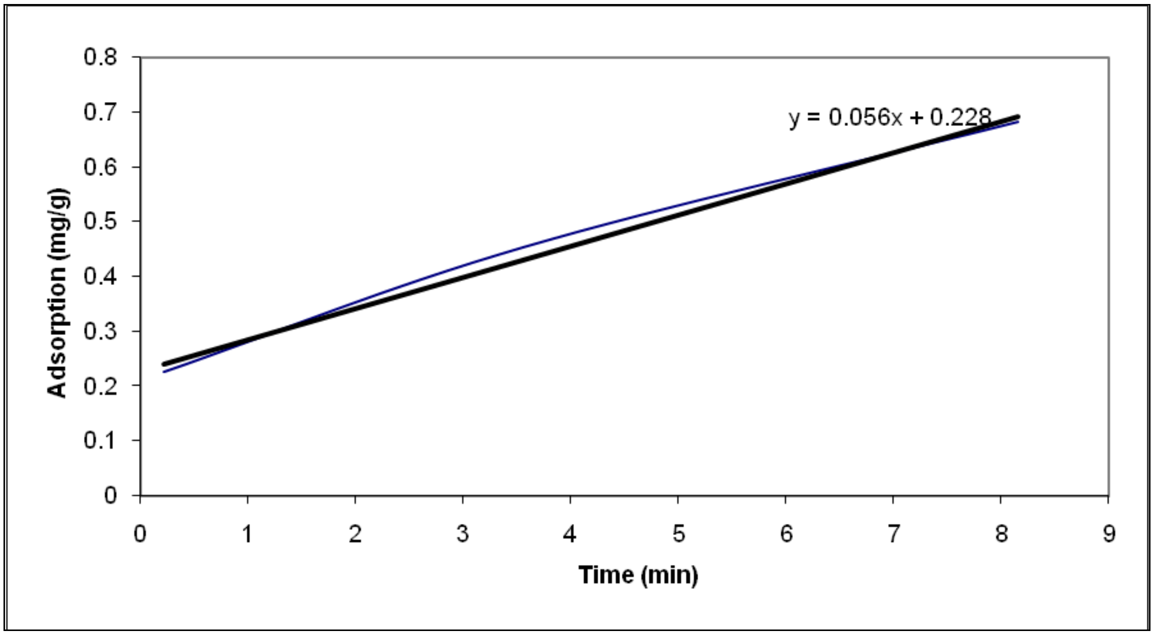

Figure 4.37: Plot of adsorption amount versus time for MA 2

Table 4.4: Initial Rates of Adsorption at 400°C for Mg-Al HTlcs

Sample	Adsorption Rates (mg/g·min)
Mg-Al HTlc (Mg/Al = 2)	0.0569
Mg-Al HTlc (Mg/Al = 3)	0.0541
Mg-Al HTlc (Mg/Al = 4)	0.0534

As shown in Table 4.4 it can be seen that the initial rates of adsorption at 400°C for Mg-Al HTlcs are similar for all molar ratios. This shows that the Mg-Al HTlcs composition does not significantly affect the initial hydrogen adsorption rate. On the other hand, for Ni-Mg-Al HTlcs, only the value for the average later rates of adsorption at 400°C can be obtained from the experimental data. The average later rate of adsorption was doubled from 0.1046 to 0.2129 mg/g.min when the Ni/Mg/Al molar ratio is increased from 1:2:1 to 2:1:1. This indicates that higher nickel content gives higher rate of adsorption at 400°C.